Sherwin Chase Department of Chemical Engineering

M. Eng. Downward two phase flow in vertical tubes

ABSTRACT

In the present work, experimental data is obtained for the amount of air entrained by water and sugar solutions, of viscosities 3.6 and 4.7 centipoises, flowing down pipes of diameters 1.0, 1.5 and 2.0 inches.

The dynamics of vapour entraining flow is discussed, and a method for calculating liquid flow rate at which pipe flows full is suggested. The experimental results have been presented in terms of some of the common dimensionless groups used in fluid mechanics in an attempt to develop an overall correlation scheme.

DOWNWARD TWO PHASE FLOW IN VERTICAL TUBES

by

SHERWIN CHASE

DOWNWARD TWO PHASE FLOW IN VERTICAL TUBES

BY

SHERWIN CHASE

Submitted to the Faculty of Graduate Studies and Research of McGill University in partial fulfillment of the requirements for the degree Master of Engineering.

Thesis Supervisor: Dr. N. E. Cooke

Department of Chemical Engineering
McGill University, Montreal, Canada March, 1971

ABSTRACT

In the present work, experimental data is obtained for the amount of air entrained by water and sugar solutions, of viscosities 3.6 and 4.7 centipoises, flowing down pipes of diameters 1.0, 1.5 and 2.0 inches.

The dynamics of vapour entraining flow is discussed, and a method for calculating liquid flow rate at which pipe flows full is suggested. The experimental results have been presented in terms of some of the common dimensionless groups used in fluid mechanics in an attempt to develop an overall correlation scheme.

ACKNOWLEDGEMENTS

The author wishes to express his gratitude to following persons who made the completion of this work possible:

To his research director, Dr. N. E. Cooke, for his assistance and guidance on this project.

To Dr. E. J. Farkas, for his co-operation in all aspects of this work.

To the academic and technical personnel of the Chemical Engineering Department for their valuable advice and service, and to fellow graduate students for their encouragement.

To his wife, for her constant encouragement and moral support.

TABLE OF CONTENTS

LIST OF TABLES

LIST OF FIGURES

INTRODUCTION

When a liquid flows down a vertical pipe under such conditions that the pipe does not flow full of liquid, some of the gas at the pipe inlet will be entrained by the flowing liquid. The gas will be compressed by the flowing liquid to a degree which depends on the ease with which the gas can escape at the bottom of the pipe. As a result of the entrainment of gas, the energy loss in the vertical pipe will be higher, and the noise and vibration in the pipe could become considerable. This flow mechanism is, therefore, an important engineering problem.

Important examples of this type of flow can be found in the take-off lines from condensers and in the seal legs at the bases of distillation columns. In the take-off lines from condensers, entrainment of vapour may cause the liquid flow rate to become uneven and the presence of air bubbles can cause oscillations in the flow meters. In seal legs at the bases of distillation columns, entrainment of vapour may cause surging in the liquid take-off which, in some cases, might be enough to blow the seal.

As a result of the induced motion of a gas by a liquid flowing down a pipe, subatmospheric pressures can be formed at the inlet of the pipe. In the drains and traps of most plumbing fixtures, the water seal is usually of the order of 1 inch. Therefore, to avoid blowing the water seal and to eliminate excessive pressure variations in the vertical stacks to which the plumbing fixtures and drains are attached, air must be supplied or removed at definite rates. Also, since gas entrained at the top of a vertical tube is carried along by the flowing liquid, the presence of entrained gas will adversely affect the performance of any centrifugal pump immediately following the vertical pipe. The effect of entrained gas must, therefore, be carefully considered in the location of centrifugal pumps in a flow system.

Two-phase flow in pipes has received considerable attention in the last twenty years, as indicated by the numerous publications available in recent literature,[1] yet the hydrodynamics can hardly be considered solved. Because of the complex nature of the flow and the differential equations describing the flow, most of the known relationships are semi-empirical in nature. Generally, these relationships have been developed from either momentum or energy balances, are usually valid only for a narrow flow region, and have been largely directed towards developing an accurate method for prediction of two-phase pressure drops. The gas entrainment problem is further complicated by the fact that the gas flow is now the important dependent variable in the analysis and, judging from the lack of information available in the literature, has received little attention.

The object of this research was to conduct an experimental study of the vapour entrainment phenomenon in order to obtain experimental results which might explain the phenomenon or which might be useful in the development of a calculation method for predicting the amount of gas which can be entrained by a flowing liquid. In systems such as the Taylor Hydraulic Compressor, in which the phenomenon has been put to practical use, this information would make accurate design possible. In those cases where entrainment of vapour is to be avoided, some design information would be available.

Experimentally, the amount of air entrained by water and two sugar solutions flowing in vertical tubes of different diameters was measured.

1 REVIEW OF LITERATURE

The entrainment of gas by a liquid flowing into a vertical pipe has long been recognized and utilized to provide compression to the gas. One of the most successful devices utilizing the phenomenon is the Taylor Hydraulic Compressor, which was first erected in 1896 by the Taylor Hydraulic Air Compressing Company of Montreal for the Dominion Cotton Mills, Magog, Quebec. The system is described in detail by Peele.[2]

In the Hydraulic Compressor, water is allowed to flow down a vertical shaft which is opened to the air at the inlet. Air is entrained and carried down the shaft by the flowing water to a large settling chamber at the bottom of the shaft where the sudden decrease in velocity (increase in area) causes the air to separate from the water. The air can be drawn off and fed to locations where it is required, while the water is fed from the settling chamber into a second vertical column. The amount of compression obtained is determined by the height of the water column, which is defined as the difference between the water level at the inlet to the shaft and the water level in the second vertical column.

In 1906, a compressed air plant of this type, having a total capacity of about 36,000 standard cubic feet per minute, was installed at the Victoria Copper Mine, Michigan. Another unit was also installed near Cobalt, Ontario which compressed 40,000 standard cubic feet per minute of air from atmospheric pressure to 120 psig.

Since the air and water flows as an intimate mixture down the shaft, the compression is isothermal and the compressed air is saturated with moisture. The efficiency of the Hydraulic Compressor, defined as a ratio of final air pressure to the liquid head available, is generally about 75%. The initial and maintenance costs of such a compressor are low compared to conventional mechanical compressors; but since the potential energy of the liquid provides the compression, extensive excavation and large quantities of flowing water are required.

Water ejectors or jet pumps have also been used to move or compress gas and provide another example of the use of the momentum of a liquid to move another fluid. The efficiencies of ejectors are usually quite low and a novel method of using a liquid to compress air has been recently investigated.[3]

The entrainment of air by flowing water presents some interesting problems in plumbing drainage systems. It is, therefore, of some interest to workers involved in the design and operation of plumbing installations and has been studied by Dawson and Kalinske.[4]

Since, in the usual plumbing installations, liquid normally flows from horizontal drain pipes into the vertical stacks, Dawson and Kalinske studied experimentally the case of water flowing down a vertical pipe from a horizontal one. On the basis of a theoretical analysis of the flow, they presented a relationship for calculating the maximum liquid velocity possible and the length of tube required to produce that velocity. For the common sizes of vertical pipes used in plumbing and industrial installations, the suggested relationship for the maximum liquid velocity is

$$V_{Lm} = (1.486/n)^{0.6} \, (Q_L/\pi D)^{0.4} \qquad (1.1)$$

where V_{Lm} is the maximum liquid velocity, and n is a constant which has been experimentally determined to be 0.006.

In their study, the amount of air entrained at various water flow rates was also measured and a method for estimating the air flow postulated. They suggested that, since the air is carried down the pipe by the flowing liquid, the maximum amount of air which can be entrained at a given liquid flow is given by the product of the maximum liquid velocity and the cross sectional area of the pipe not occupied by the liquid. The maximum air flow for any liquid flow is therefore given by

$$Q_{Am} = (\pi D^2/4 - Q_L/V_{Lm})\, V_{Lm} \qquad (1.2)$$

They also concluded, on the basis of their experimental evidence, that

(i) subatmospheric pressures are formed in the entrance region of the vertical pipe,

(ii) the maximum subatmospheric pressure is formed at a short distance below the water entrance, and

(iii) the maximum liquid velocity is reached within a few feet of the pipe entrance.

By considering the flow of an elemental disc of water at any distance L below the point of entry into the vertical pipe, Dawson and Kalinske postulated that the acceleration of the element will be given by the difference between the gravitational force on the element and the frictional force at the wall of the pipe. Since, for the maximum liquid velocity, the liquid acceleration is zero, they were, therefore, able to develop equation (1.1) to describe the flow in their system. They had also suggested that such a theoretical analysis should be valid for systems with a different entrance geometry, e.g., flow from a tank into a vertical pipe, as long as the pipe does not flow full. On the basis of the results obtained (Tables A.1, A.2, A.3) when equations (1.1) and (1.2) are applied to the experimental results obtained in the present study, these equations obviously do not apply to flow in the 1.0 and 1.5 inch diameter pipes. This, therefore, means that equations (1.1) and (1.2) are not generally valid, but are perhaps approximately accurate for 3, 4, and 6 inch pipes as experimentally studied by Dawson and Kalinske.

The most complete study of the hydraulics of vertical drain and overflow pipes was presented by Kalinske.[5] A drain pipe is defined as one which is connected flush with a horizontal surface such as the bottom of a tank, and an overflow pipe is one which extends an appreciable distance into the tank.

The experimental work was concerned with the hydraulic and pneumatic conditions when water entered vertical pipes of diameters 1.7, 3.7, and 5.8 inches, having squarecut edges at the entrance, under such low heads that the pipes did not flow full and air was drawn down into the pipes. The main purpose of the experimental work was to develop a head-discharge relationship and to determine the effect of pipe length on such a relationship. Some data on the amount of air drawn by the flowing water was also presented. This work indicates that

(i) the air flow increases with pipe length, the rate of increase in air flow becoming less with longer pipe lengths,

(ii) there is no significant difference in air flows between drain and overflow pipes, and

(iii) subatmospheric pressures are formed just below the pipe entrance.

Laushey and Mavis,[6] in an effort to relate entrance conditions and air entrainment, measured the amount of air entrained by water flowing down Lucite shafts of diameters 2.8 and 5.6 inches. They investigated two different types of entrances, radial entrance and spiral (vortex) entrance, as indicated in Figure (1.a), and observed some difference in air flows in the two cases.

For spiral entrance, no negative pressures were observed anywhere in the shaft and a direct correlation between air-water ratio and distance from the inlet to the hydraulic grade line in the shaft was obtained. For radial entrance, negative pressures were observed and there was no direct correlation between air-water ratio and distance to hydraulic grade line.

For single phase flow in pipes, the hydraulic grade line is defined as that line which is always a distance $(P/\rho g + Z)$ vertically above a horizontal datum, or at a distance $(V^2/2g)$ below the total energy line. For flow down a vertical tube, the distance from the tube inlet to the hydraulic grade line should be given by $(V^2/2g)$, which suggests that for spiral entrance there is a direct correlation between the air-water ratio and a Froude Number of the liquid. Because it is not very clear from the work of Laushey and Mavis how the distance to the hydraulic grade line has been measured or determined, no significant conclusions can be drawn from their study at this time. The relationship obtained for spiral flow was given by

$$Q_A / Q_L = 0.015\ Y \qquad (1.3)$$

where Y is the distance in feet from the pipe inlet to the hydraulic grade line.

Radial entrance

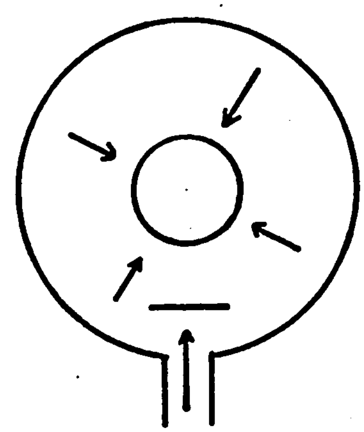

Spiral entrance

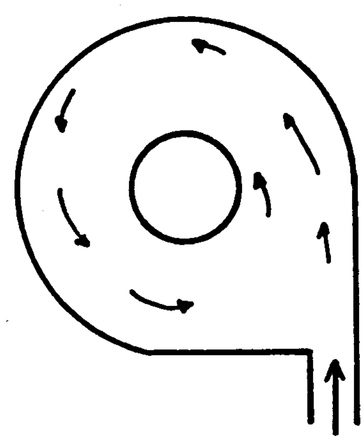

FIGURE 1-a Systems studied by Laushey and Mavis

No method of calculating or predicting the amount of vapour which can be entrained by a liquid flowing down a vertical pipe has ever been presented in the literature, and reliance has been placed on experimental models as a means of predicting flows.

The problems of scaling up air measurements taken in the models are still unsolved in spite of the many attempts which have been made. Two references on the subject are the works of Hall[7] and Peterka.[8]

Hall described the modelling of the drop shaft at the San Pablo dam in which the air flow was quite different from that in the model. Peterka reported that a 1:21.5 model of the Hearte Butte bellmouth spillway underestimated the air-water ratio by a factor of four, although it accurately predicted the water flow.More recently, the Hydraulics Research Station, Wallingford tested three models of a vertical drop shaft to scales 1:10, 1:20, and 1:30 in an attempt to relate air entrainment with model scale, but no general result emerged from the work. This lack of success was reported by Binnie and Simms[9] who, in an attempt to test an hypothesis suggested by Williamson and Naylor among others, measured air entrainment by flowing water under reduced atmospheric pressure.

Williamson[10] and Naylor[11] had suggested that more accurate modelling of air entraining flow might be possible if the ambient pressure was reduced in conformity with the linear scale, thus maintaining the absolute pressure on an air bubble correctly. Binnie and Simms, however, concluded from their study that any attempt to predict air entrainment from measurements from a model at reduced ambient pressure would be even more inaccurate than the normal atmospheric pressure models. They noted that the effect of reducing the ambient pressure from atmospheric pressure (30 inches of mercury) to 2 inches of mercury was to reduce the air discharge by about one-sixth, while there was no effect on the head-discharge relationship.

2 DYNAMICS OF VAPOUR ENTRAINING FLOW

2.1. Flow regimes in downward vertical pipe flow

When a liquid flows down a vertical pipe which is initially empty, different flow regimes exist. On the basis of experimental evidence, these regimes can be simply described as

(i) simple weir flow,

(ii) vapour entraining flow, and

(iii) full pipe flow.

The existence of different flow regimes for flow down a vertical pipe has been suggested by Binnie[12] and it is reasonable to expect that transition from one regime to another is not a definite phenomenon.

A typical head-discharge curve showing the possible flow regimes is presented in Figure (2.a) and it indicates that there is some minimum liquid flow rate required before vapour is drawn down the pipe. The existence of regime (i) has been postulated on the basis of experimental evidence, since it has been observed from the experimental results available (References (4), (8) and the present study) that graphs of air flow against liquid flow do not pass through the origin.

Regime (i), which corresponds to very low head/liquid flow rates, should be only a very minor effect in the overall picture; but no conclusive reasons for the existence of the regime can be suggested here. For increasing liquid flow rates, vapour is entrained until the pipe flows full of liquid, at which point there is a sudden rise in the head-discharge curve, as indicated in Figure (2.a). At liquid flow rates approaching that required to fill the pipe, entrainment of vapour becomes unsteady and the whole vapour entrainment becomes even more complex in this transition region.

After the pipe starts to flow full of liquid, further increase in the head of liquid above the pipe entrance does not appreciably increase the rate of discharge. In this regime, the head-discharge relationship is simply that for ordinary pipe flow with a sharp-edged entrance. In some cases, if the pipe is short, the liquid flow springs from the wall leaving an air space between the wall and the liquid and emerges as a glassy jet.

Anwar[13] and Kalinske[4] have measured coefficients of discharge for the full pipe flow regime. A suitable value

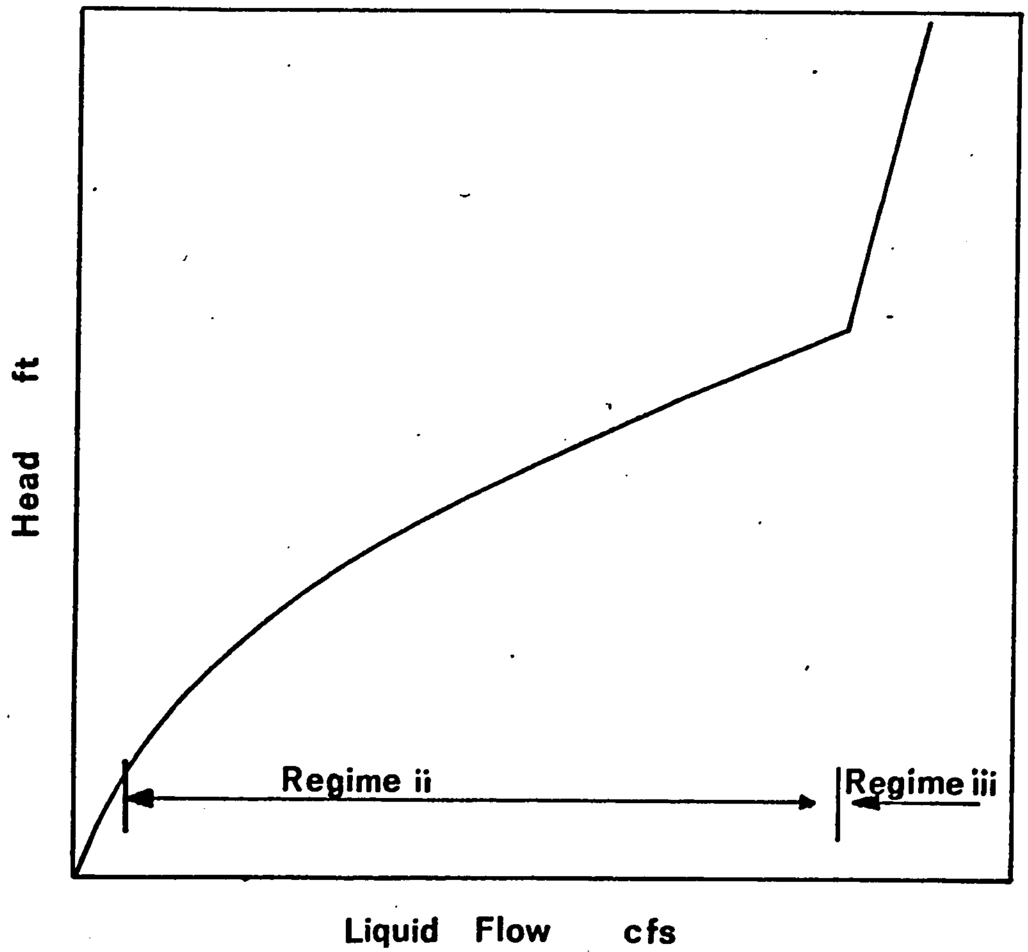

Figure 2·a Typical Head – Discharge Curve of this coefficient lies between 0.5 and 0.61 for drain pipes, i.e., pipes connected flush with a horizontal surface, while for overflow pipes the value is 0.7.

2.2. The vapour entraining flow regime.

When the liquid level in a tank, to which a vertical outlet pipe is connected, is lowered, a dimple forms on the surface of the liquid. If the tip of the dimple reaches the mouth of the outlet pipe, the vapour above the liquid will be drawn down into the outlet pipe.

In some cases, this dimple grows into a vortex, longitudinal in shape and with radius decreasing in the direction of the outflow opening. The vortex usually pulsates as the tip comes near to the entrance of the outlet pipe and entrainment of vapour should begin when the tip of the vortex passes the point of greatest contraction of the jet in the top of the outlet pipe. Entrainment of vapour is usually accompanied by clearly audible sounds, and, for a given discharge of liquid from a tank, should begin at a definite level in the tank.

The liquid level at which air entrainment starts has been investigated experimentally and theoretically by Harleman et al.,[14] Lubin and Springer[15] and Gluck et al.[16] It is interesting to note that, even though Lubin and Springer made no reference to the work of Harleman et al., the agreement between the two studies is good. A typical flow arrangement is shown in Figure 2.B. and a brief summary of the above studies[14], [15], [16] is presented below.

Harleman et al. investigated a system with a well defined interface between liquids of similar viscosities but different densities. On the basis of inviscid, incompressible, irrotational flow, the analytical expressions developed were:

$$g^1 = g(1 - \rho_1/\rho_2) \qquad (2.1)$$

$$V_c = 4Q_L / \pi D^2 \qquad (2.2)$$

$$V_c/(g^1 h_o)^{0.5} = 3.20\ k(h_o/D)^2 \qquad (2.3)$$

From the experiments, k was found to be a constant equal to 0.64 and the final expression presented by Harleman et al. was

$$V_c /(g^1 h_o)^{0.5} = 2.05\ (h_o /D)^2 \qquad (2.4)$$

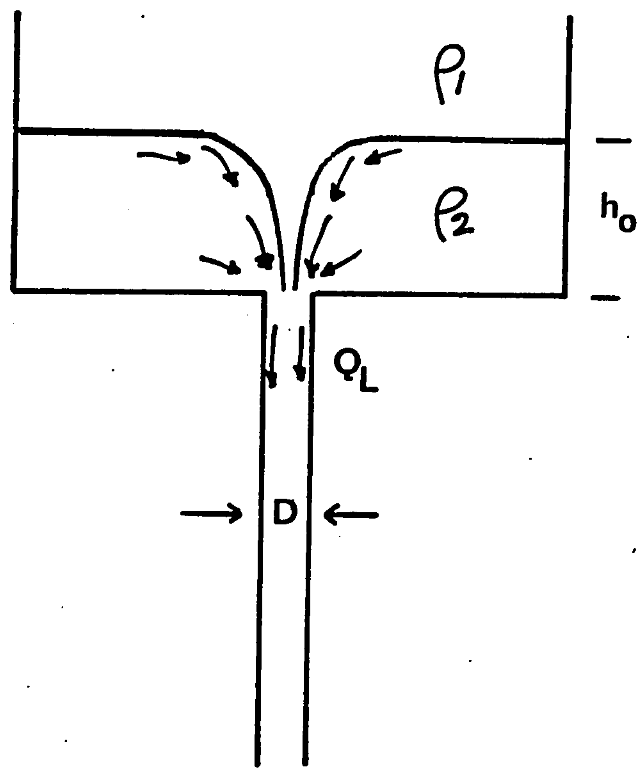

Figure 2-c Vapour entrainment just started

Liquid-liquid and air-water systems were investigated by Lubin and Springer and the relationship between h_o and liquid flow rate was given by

$$(h_o/D) = 0.69 \left[Q_L^2 / (1 - \rho_1/\rho_2) \, gD^5 \right]^{0.2} \quad (2.5)$$

where 0.69 was the constant determined from the experimental results.

By using equations (2.1) and (2.2), equation (2.4), as obtained by Harleman et al., reduces to

$$(h_o/D) = 0.83 \left[Q_L^2 / (1 - \rho_1/\rho_2) \, gD^5 \right]^{0.2} \quad (2.6)$$

The agreement between the results of Harleman et al. and those of Lubin and Springer is obvious from the form of equations (2.5) and (2.6).

Gluck et al. were concerned with determining the relationship between gas ingestion height and other parameters of flow. The gas ingestion height is defined as the height of liquid in the tank at which gas is first drawn down the outlet pipe by the flowing liquid, and is therefore equivalent to h_o in equations (2.5) and (2.6).

Gluck et al. observed that, even in the absence of swirl of the liquid, the phenomenon of gas ingestion occurs, and, on the basis of their experimental results, suggested a relationship for the gas ingestion height of the form

$$(h_o / D) = 0.43 \tanh (1.3V_o^2/gD)^{0.29} \qquad (2.7)$$

where V_o = interface velocity of the liquid in the tank.

The usefulness of equation (2.7) for giving an operating estimate of the minimum height of liquid in a tank is limited since V_o is not usually or easily measured. Equations (2.5) or (2.6) are more useful for providing such an estimate; but, since the experiments(14) show that there is a marked influence of liquid surface disturbances on the value of h_o, the value of liquid height predicted by equations (2.5) or (2.6) will be the lowest possible height which should be maintained if gas is not entrained.

2.3. Prediction of full pipe flow.

As discussed in Section 2.1, vapour is entrained by the flowing liquid unless the pipe flows full of liquid. The liquid flow rate at which the pipe first flows full, therefore, represents the upper limit of vapour entrainment and should be a useful parameter for the flow.

By assuming that, when the pipe flows full there is negligible swirl, a simple method for calculating the liquid flow rate for full pipe flow can be developed.

For a pipe flowing full of liquid:

Total head loss = exit + entrance losses + friction loss (2.8)

$$\text{entrance loss} = C_i \cdot v^2/2g \tag{2.9}$$

$$\text{exit loss} = C_o \cdot v^2/2g \tag{2.10}$$

$$\text{friction loss} = 4f \cdot L/D \cdot v^2/2g \tag{2.11}$$

If h_c = height of liquid above outlet pipe when pipe first flows completely full,

Q_{LF} = liquid flow rate when pipe first flows full.

$$\text{Total head loss} = h_c + L \tag{2.12}$$

$$(h_c + L) = (C_i + 4f \cdot L/D + C_o)\, v^2/2g \tag{2.13}$$

From the data of Kalinske[4] and Anwar,[13] a reasonable value for $C_i = 0.55$.

$C_o = 1$ and, since $h_c + L \simeq L$, i.e. $h_c \ll L$

$$L = (1.55 + 4f \cdot L/D)\, v^2/2g \tag{2.14}$$

$$Re_F = \frac{4 \rho_L Q_{LF}}{\pi \mu_L D} \tag{2.15}$$

From (2.14),
$$f = \frac{2gD}{4v^2} - \frac{1.55D}{4L} \tag{2.16}$$

$$\therefore \quad f = \frac{\rho_L^2 g D^3}{2 \mu_L^2} \cdot \frac{1}{Re_F^2} - \frac{1.55D}{4L} \tag{2.17}$$

For flow in circular pipes, Drew[17] has derived a relationship between friction factor and Reynolds number of the form

$$f = 0.0014 + 0.125 \, Re^{-0.32} \qquad (2.18)$$

Solving equations (2.17) and (2.18) will, therefore, give the value of the Reynolds number at which the pipe first flows full (Re_F). Equations (2.17) and (2.18) are non-linear and a graphical method was used to solve the equations.

2.4. Semi-theoretical analysis of flow.

Since the amount of vapour entrained by a flowing liquid must be an indication of the amount of momentum transferred from the liquid to the vapour, a complete analysis of the velocity profiles in the liquid would be required to give a fundamental explanation of the phenomenon.

The liquid supply line and inlet tank in Kalinske's experimental apparatus had been designed to eliminate swirl in the liquid as it flowed into the outlet pipe; but it was observed that vortex flow developed in all cases except those where the pipe was very short (2 feet or less). In the study described in this thesis, a design for eliminating swirl, which was different from the flow arrangement of Kalinske, was adopted; but again vortex flow developed in all the cases studied. Haindl,[18] in his study of the contribution of a vortex to air entrainment, concluded that general movement of the liquid surface may be enough to cause a circulation impulse which would result in a vapour entraining vortex. From these observations, one would conclude that, under conditions of vapour entrainment, some sort of vortex flow will always exist at the top of the pipe.

The formation of a vortex is a complex phenomenon and all of the factors necessary to achieve a complete theoretical analysis have not been fully explained, even though many theoretical studies[27-30] have been made; but, as shown in the work of Anwar,[19] the results of many of these studies of vortex flow are not directly applicable to systems such as the one being investigated. Because of the obvious complexity of the flow, a satisfactory theoretical analysis was not possible in this study and, instead, an attempt has been made to present the graphical relationships between the experimental measurements and some of the usual parameters of flow systems. It has been observed that the entrained vapour flows in the central core of the pipe, while the liquid flows as a thin film along the walls of the pipe and, therefore, a theoretical analysis of the annular flow regime in the pipe has been attempted.

2.4.1. Estimation of size of air core.

The existence of a universal velocity distribution equation in terms of two parameters u^+ and y^+, which are defined in equation (2.19), has been suggested by Von Karman[20] and verified by the data of Nikuradse.[21] On the basis of the experimental results of Nikuradse, expressions for velocity distribution for full pipe flow, as given in equations (2.21) to (2.23), have been developed.

It has been argued[22] that, in the case of annular two phase flow, the liquid in the film below the interface is unable to distinguish between an adjacent shear which has been transmitted ultimately from a liquid or gas source moving as a center core. Dukler and Bergelin[22] further argued that, if one imagines that the gas core is replaced by a liquid stream moving with such a velocity distribution that the interfacial shear is unchanged, it seems reasonable to apply equations (2.21) to (2.23) to the liquid film flowing along the wall, as long as the remaining conditions under which those equations were developed were not violated. In pipes flowing full, velocity gradients in the turbulent core are not large and, therefore, equations (2.21) to (2.23) would be inaccurate in describing falling films with large interfacial shear. As a result of such considerations, workers in two phase flow, such as Dukler and Bergelin[22], Anderson and Mantzouranis[23], and Levy[24], have used equations (2.21) to (2.23) to describe the flow in liquid films, and have obtained reasonable correlations for their experimental results.

In order to obtain some estimate of the size of the air core in the present study, it will be assumed that the velocity distribution in the liquid film can be represented by the equations (2.21) to (2.23). In the present system, movement of the air results from the momentum transferred from the liquid to the air as the liquid flows into the top of the tube. If it is postulated that the air is accelerated from rest to some average velocity in the top of the tube and flows down the tube without being further accelerated to any appreciable degree, we can define the motion of the liquid film by a balance between shear force at the wall and the gravitational force on the liquid. On the basis of these postulates, a value for the diameter of the air core can be obtained by the analysis which follows.

The parameters u^+ and y^+ are defined in terms of a characteristic velocity u^*, called the friction velocity, which is related to the wall shear stress by equation (2.24).

$$u^+ = u/u^* \tag{2.19}$$

$$y^+ = \rho_L y u^* / \mu_L \tag{2.20}$$

For $0 < y^+ < 5$,

$$u^+ = y^+ \tag{2.21}$$

For $5 < y^+ < 30$,

$$u^+ = 5.0 \ln y^+ - 3.05 \tag{2.22}$$

For $30 < y^+ < y_i^+$,

$$u^+ = 5.5 + 2.5 \ln y^+ \tag{2.23}$$

$$u^* = (\tau_W / \rho_L)^{0.5} \tag{2.24}$$

Since y is the distance in the film measured from the wall of the pipe,

$$y = R - r \tag{2.25}$$

The volumetric liquid flow rate is given by

$$Q_L = 2\pi \int_{r_i}^{R} ru \, dr \tag{2.26}$$

$$dr = - dy \tag{2.27}$$

When $r = R$, $y = 0$, and when $r = r_i$, $y = y_i$.

$$\therefore \; Q_L = 2\pi \int_0^{y_i} (R - y)\, u^* u^+ \, dy \tag{2.28}$$

Substituting equation (2.20) in equation (2.28), the expression for liquid flow becomes

$$Q_L = \frac{2\pi R \mu_L}{\rho_L} \int_0^Y u^+ \, dy^+ - \frac{2\pi \mu_L}{u^* \rho_L^2} \int_0^Y u^+ y^+ \, dy^+ \qquad (2.29)$$

where Y is the value of y^+ at the interface.

Since u^+ is a different function of y^+ for different ranges of values of y^+, a single expression for Q_L is not obtained, as suggested in some previous publications[22][23]. Instead, liquid flow rate is given by the equations (2.30) to (2.32) within the limits indicated.

For $Y < 5$,

$$Q_L = \frac{2\pi R \mu_L}{\rho_L} \cdot \frac{Y^2}{2} - \frac{2\pi \mu_L^2}{u^* \rho_L^2} \cdot \frac{Y^3}{3} \qquad (2.30)$$

For $5 < Y < 30$,

$$\begin{aligned} Q_L = {} & (2\pi R \mu_L / \rho_L)(5.0Y \ln Y - 8.05Y + 12.54) \\ & - (2\pi \mu_L^2 / u^* \rho_L^2)(2.5 Y^2 \ln Y - 2.78Y^2 + 10.37) \end{aligned} \qquad (2.31)$$

For $Y > 30$

$$\begin{aligned} Q_L = {} & (2\pi R \mu_L / \rho_L)(2.5 \ln Y + 3.0Y - 64.04) \\ & - (2\pi \mu_L^2 / u^* \rho_L^2)(1.25Y^2 \ln Y + 2.13Y^2 - 573.2) \end{aligned} \qquad (2.32)$$

For steady state flow of the liquid, considering that the interfacial shear has negligible influence on the liquid film as discussed on page 27, and that the pressure in the inlet tank and at the bottom of the pipe is atmospheric,

$$\tau_W = \rho_L \, g(R^2 - r_i^2)/2R \qquad (2.33)$$

$\therefore$ From equation (2.24),

$$u^* = (g \, (R^2 - r_i^2)/2R)^{0.5} \qquad (2.34)$$

From equation (2.20),

$$Y = \rho_L \, (R - r_i) \, u^* / \mu_L \qquad (2.35)$$

From equations (2.34), (2.35) and either (2.31), (2.32) or (2.33), a relationship between Q_L and r_i is now available. Because of the obvious non-linearity of the equation, which would result by combining the equations (2.31) to (2.35), no attempt will be made to solve such an equation directly but, instead, values of Q_L , r_i will be generated to provide a plot of r_i against Q_L from which the size of the air core, corresponding to each experimental liquid flow rate, can be determined. A typical plot, as obtained from water, is presented in Figure (2.1).

Dukler[26] has presented a theoretical analysis for a liquid film flowing down a vertical tube, in which he defines a parameter β which characterizes the interfacial shear.

If β in this case is defined by

$$\beta = \left(\rho_A D / \rho_L)(g \left(\rho_L / \mu_L\right)^2\right)^{0.33} \qquad (2.36)$$

values of Re_L and (d_a/D) can be calculated for the different values of β for each system studied. These values of β are shown in Table (2.1), and a plot of (d_a/D) against liquid Reynolds number (Re_L) has been presented in Figure (2.2).

TABLE 2.1

Liquid	Pipe diameter (ins.)	β
Water	2.0	1.31
	1.5	0.98
	1.0	0.65
Sugar Solution 1	2.0	0.55
	1.5	0.41
	1.0	0.27
Sugar Solution 2	2.0	0.45
	1.5	0.34
	1.0	0.22

GRAPH OF d_a/D vs Q_L

AIR - WATER SYSTEM

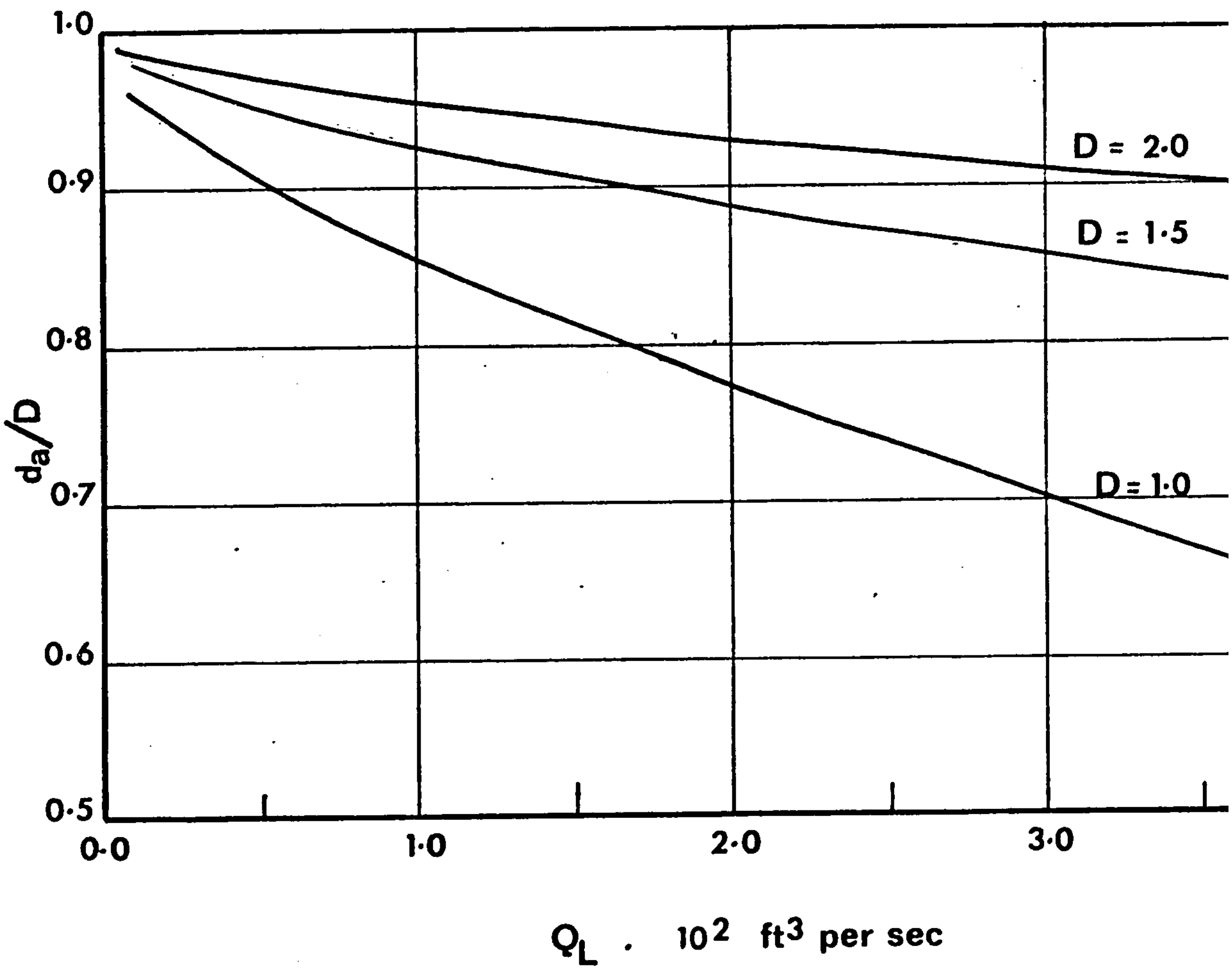

FIGURE 2·1

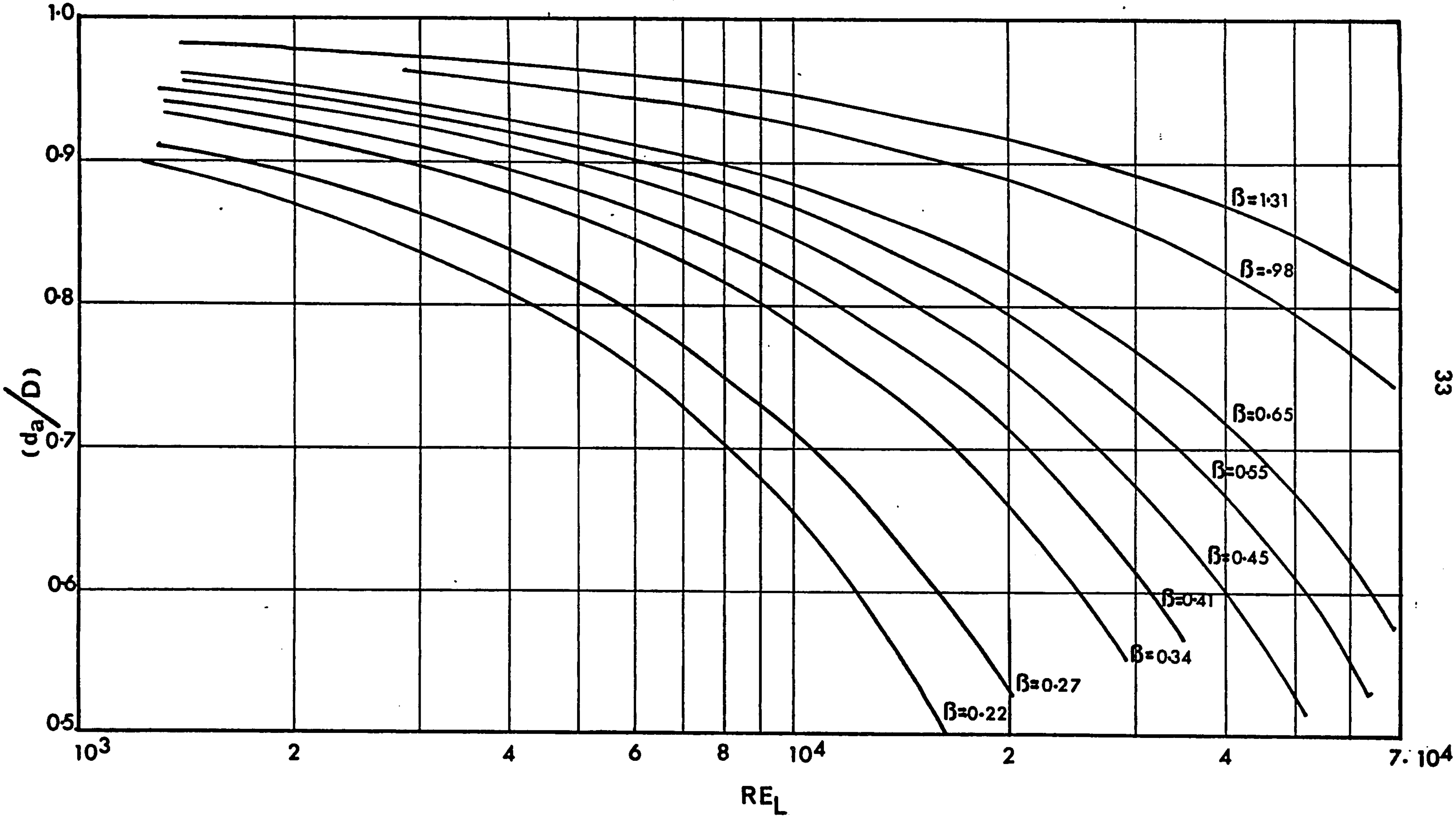
1·0
0·9
0·8
0·7
0·6
0·5
(d_a/D)
10^3
2
4
6
8
10^4
2
4
$7 \cdot 10^4$
RE_L
ß=1·31
ß=·98
ß=0·65
ß=0·55
ß=0·45
ß=0·41
ß=0·34
ß=0·27
ß=0·22

FIGURE 2·2

2.5. Dimensional analysis of flow.

2.5.1. Using the more general dimensionless groups.

Since the equations describing the flow in the present system are too complex to be solved by normal methods, an attempt will be made to use dimensional analysis to indicate either the possible relationships between the variables involved or the dimensionless groups which might provide correlations for the experimental results. By considering the important variables in the system, the air flow should be given by

$$Q_A = K\,(Q_L,\ \mu_L,\ \rho_L,\ D,\ L,\ \mu_A,\ \rho_A,\ g,\ \sigma_L) \qquad (2.37)$$

In the systems studied, μ_A, ρ_A, L were always constant and equation (2.37) reduces to

$$Q_A = K_1\,(Q_L,\ \mu_L,\ \rho_L,\ D,\ \sigma_L,\ g) \qquad (2.38)$$

where K_1 can now be considered to include ρ_A, μ_A, L. There are 7 variables, and 3 fundamental dimensions (mass, length, time). Therefore, there should be 4 dimensionless groups necessary to describe the system.

By using either the Rayleigh method or the

Buckingham Pi method, it is theoretically possible to derive dimensionless groups involving the variables in equation (2.37). Some of the more familiar groups, involving the above quantities, are the Reynolds number, the Froude number and the Film number (K_F)[25], and, using these groups, a possible relationship can be suggested. By definition:

Reynolds number, $$Re_L = 4\,\rho_L Q_L / \pi \mu_L D \qquad (2.39)$$

Froude number, $$Fr_{LT} = V_{LT} / (gD)^{\frac{1}{2}} \qquad (2.40)$$

Film number, $$K_F = g\mu_L^4 / \rho_L \sigma_L^3 \qquad (2.41)$$

$$V_{AT} = (4Q_A / \pi D^2) \qquad (2.42)$$

$$Fr_{AT} = V_{AT} / (gL)^{\frac{1}{2}} = 4Q_A / \pi D^2 (gL)^{\frac{1}{2}} \qquad (2.43)$$

$$Re_{AT} = (4\,\rho_A Q_A / \pi \mu_A D) \qquad (2.44)$$

$\therefore$ possible functional relationships for the air flow may be

$$\phi_1 (\,Re_{AT},\ Re_L,\ Fr_L,\ K_F\,) = 0 \qquad (2.44a)$$

or, since in this case ρ_A, μ_A, L are all constant, the functional relationship may be given by

$$\phi_2 (\,Fr_{AT},\ Re_L,\ Fr_L,\ K_F\,) = 0 \qquad (2.44b)$$

The Film number (K_F), values of which are shown in Table 2.2, simply represents the physical properties of the liquids and, since only three liquids were tested, the Film number (K_F) must be considered a minor correlating group. It should be possible to obtain a relationship between air flow and liquid flow by plotting graphs involving the groups in equations (2.44a) and (2.44b).

TABLE 2.2

Liquid	Film number (K_F)
Water	1.37×10^{-11}
Sugar Solution 1	5.48×10^{-9}
Sugar Solution 2	1.40×10^{-8}

Graphs of Fr_{AT} and Re_{AT} vs Re_L have been presented in Figures (A.1) to (A.4) for some of the experimental data, and show that all the experimental data cannot be adaquately correlated by a single curve by the use of such groups. Figures (A.1) to (A.4) indicate that, even if the liquid Reynolds number (which includes the major physical properties of the liquid) is specified, the resulting air flow will not be uniquely specified by the Froude or Reynolds number of the air.

These graphs may be considered to be plots of Fr_{AT} or Re_{AT} vs Re_L, having β as a parameter where, for each air-liquid system, the family of curves is adequately represented in terms of the β parameter. The lateral spread between the curves for the air-water system and the air-sugar solutions systems may be considered due to variation in the value of K_F. From Figure (A.4), it is seen that the experimental data for the two sugar solutions may be represented by graphs having β as a parameter (except for the curve for solution 2 in the 2-inch pipe), thus indicating that the effect of the film number K_F is not appreciable in the case of the sugar solutions.

2.5.2. Using the size of the air core.

When using dimensional analysis to obtain a possible relationship between a dependent variable and several independent variables, the task is often simplified if a functional relationship between some of the dependent variables and any second variable or variables, on which the dependent variable must depend, can be found. In this case, the air flow must obviously depend on the size of the air core in the pipe. Reynolds or Froude number, based on the diameter of the air core, should, therefore, be more representative of the air flow than Fr_{AT} or Re_{AT}, and new dimensionless numbers can be defined.

By definition,

$$Re_A = (4 \rho_A Q_A / \pi \mu_A d_a) \tag{2.45}$$

$$Fr_A = V_A / (g d_a)^{\frac{1}{2}} \tag{2.46}$$

$$V_A = (4 Q_A / \pi d_a^2) \tag{2.47}$$

$$Fr_L = V_L / (gD)^{\frac{1}{2}} \tag{2.48}$$

$\therefore$ possible functional relationships for the air flow are

$$\phi_3 (Fr_A, Re_L, Fr_L, K_F) = 0 \tag{2.49}$$

or, since L, ρ_A, μ_A are constant for all the experiments, we may write

$$\phi_4 (Re_A, Re_L, \beta, K_F) = 0 \tag{2.50}$$

Graphs of Re_A vs Re_L have been presented in Figures (A.5) and (A.6), but such plots show no significant improvement over the correlation obtained in Figures (A.1) to (A.4), and show that there is no unique relationship between Re_A and Re_L.

2.5.3. Using the velocity of liquid at the interface.

The groups suggested in equations (2.45), (2.46), (2.49) and (2.50) do not give a sufficiently general correlation for air flow and a more fundamental parameter of the flow system might give an improvement over the preceding attempts. The air flow is the result of transfer of momentum from the liquid to the air across the liquid-air interface and, therefore, a group involving the liquid interface velocity might be useful in explaining the experimental data. An interface velocity can be calculated from equations (2.21), (2.22) or (2.23) and a possible method of correlation, based on the liquid interface velocity, can be suggested by the simple analysis which follows.

Momentum of air leaving tube, $M_A = (\rho_A V_A^2 \pi d_a^2/4)$ (2.51)

i.e. momentum transferred by liquid $= M_A = (\rho_A V_A^2 \pi d_a^2/4)$ (2.52

If we say that an ideal amount of momentum is transferred when the average velocity of air $= V_1 / 2$, then ideal amount of momentum transferred (M_I) will be given by

$$M_I = (\rho_A V_1^2 \pi d_a^2/16) \qquad (2.53)$$

$\therefore$ an efficiency of momentum transfer (E_m) can be defined

$$E_m = M_A / M_I = 4(V_A / V_i)^2 \qquad (2.54)$$

By definition, $$Re_I = (\rho_L V_i D/\mu_L) \qquad (2.55)$$

It seems reasonable that E_m, and hence (V_A/V_i), should be a function of Re_I, Re_L, etc. and, therefore, plots involving $(V_A / V_i)^2$, Re_I, Re_A, Re_L could possibly provide a general correlation method for the experimental data. Graphs using these groups have been presented in Figures (A.7) and (A.8). These graphs again indicate that there is no unique relationship between air flow and liquid flow rate, and that, in order to predict the air flow rate at a given liquid flow rate, other parameters (at the present unknown) will have to be specified.

2.5.4. Using other methods.

It seems likely that, as the air core becomes smaller, there is greater resistance to flow. This could be due to disturbances of the liquid surface and, by analogy with pipe roughness in single phase flow, will be considered as a first approximation to be given by $k_2 (D - d_a)/d_a$.

If we assume that the air flow can be represented by

$$Re_A = k_1 Re_L^2 - k_2 (D - d_a)/ d_a \cdot Re_L \quad (2.56)$$

then k_1 and k_2 can be determined by a method of least squares. Typical results as for air-water data in a 2.0 inch pipe are shown in Table (A.13) and show that equation (2.56) is not suitable for correlating the experimental results.

Any equation describing the air flow should satisfy two conditions:

(i) air flow is zero for approximately zero liquid flow.

$$\text{When } Q_L = 0, \quad Q_A = 0 \quad (2.57)$$

(ii) when pipe flows full of liquid, air flow is zero.

$$\text{When } Q_L = Q_{LF}, \quad Q_A = 0 \quad (2.58)$$

One possible equation for air flow is, therefore,

$$Q_A / Q_L = a \cdot (Q_L / Q_{LF})^b \cdot (1 - Q_L / Q_{LF})^c \quad (2.59)$$

An indication of the suitability of equation (2.59) would be the accuracy with which it fits the experimental data. The experimental results have been expressed in this form by a multiple linear regression analysis and the values of a, b, and c, as well as the accuracy of fit determined.

Equation (2.59) has been found to fit the experimental results reasonably well, but no general conclusions can be drawn concerning the dependence of a, b, and c on the parameters of the system. The values of a, b, and c are shown in Table (A.14).

3 DETAILS OF EXPERIMENTS

3.1. Introduction.

The experiments were carried out to determine the amount of air entrained by liquids of different physical properties flowing down pipes of various diameters.

The pipes, which were made of a transparent plastic, were all 12 feet in length and were of diameters 1.0, 1.5 and 2.0 inches. The flowing liquids were water and two sugar solutions of viscosities 3.6 and 4.7 centipoises.

3.2. Description of apparatus.

The experimental equipment, in which the liquid flows in a closed cycle, is shown in Figure (3.A).

Liquid from the storage tank (t) was supplied to the inlet tank (i) by the centrifugal pump (p), and measured by an orifice plate incorporated in a 1.5 inch-diameter vertical tube. For precise measurement over a large range of liquid flows, two different sizes of orifices were used. The orifice plates, which were connected to a mercury manometer, were of diameters 0.5 and 0.992 inches and were calibrated using the calculation method described in [31].

The inlet tank was a completely sealed rectangular box of dimensions 16" x 16" x 6", made of clear acrylic plastic. Liquid was introduced into the tank through a 2-inch diameter opening in the side of the tank, and the outlet, to which pipes of different diameters could be attached, was centrally placed in the bottom face of the tank.

A U-tube manometer (m), using water or a light oil as the fluid, was connected to the inlet tank and was used to give an indication of the air pressure in the tank. One arm of the manometer was always open to the atmosphere and, therefore, the pressure indicated by the manometer was always relative to atmospheric pressure.

To eliminate swirl and obtain symmetrical flow of liquid into the test pipe, a system of baffles was attached to the inside bottom face of the tank.

The system, which was symmetrical about the outlet, consisted of four baffles, each 12" in length and 4" high, arranged in the form of a rectangle plus a circular baffle

7" in diameter and 2.5" high. As the liquid entered the tank, it flowed over the rectangular baffle arrangement and then over the circular baffle before entering the test pipe.

This design effectively eliminated swirl in the liquid as it flowed into the top of the tube and was effective in reducing the momentum of the liquid when it entered the tank.

The air, which was available at 100 - 120 psig, was supplied to the inlet tank via two pressure regulators. The first regulator was capable of a delivery pressure of 2 - 6 psig, while the second regulator could be manually controlled to maintain atmospheric pressure in the inlet tank.

The air flow was measured by a Precision Wet Test Meter(W.T.M.) and/or two Lo-Flow gas rotameters(r_1, r_2), which were connected in a parallel flow arrangement. When using the Wet Test Meter to measure gas flow, the pressure of the flowing gas is always indicated by the water manometer which is an integral part of the device. It was, therefore, quite simple to maintain a close check on the air pressure in the inlet tank.

3.3. Experimental method.

To take a measurement, the liquid flow rate was set to the required value by adjusting the globe valve in the outlet line from the centrifugal pump, and air was supplied to the inlet tank at such a rate as to maintain the air pressure in the tank at atmospheric.

Since one arm of the manometer (m) was open to the atmosphere, the pressure in the tank is atmospheric when the liquid level in each arm of the manometer is the same. In the apparatus, the bottom of the test pipe was always exposed to atmospheric pressure, and the air was supplied to the inlet tank at atmospheric pressure. The measured amount of air supplied to the tank must be the amount of air which is entrained by the flowing liquid.

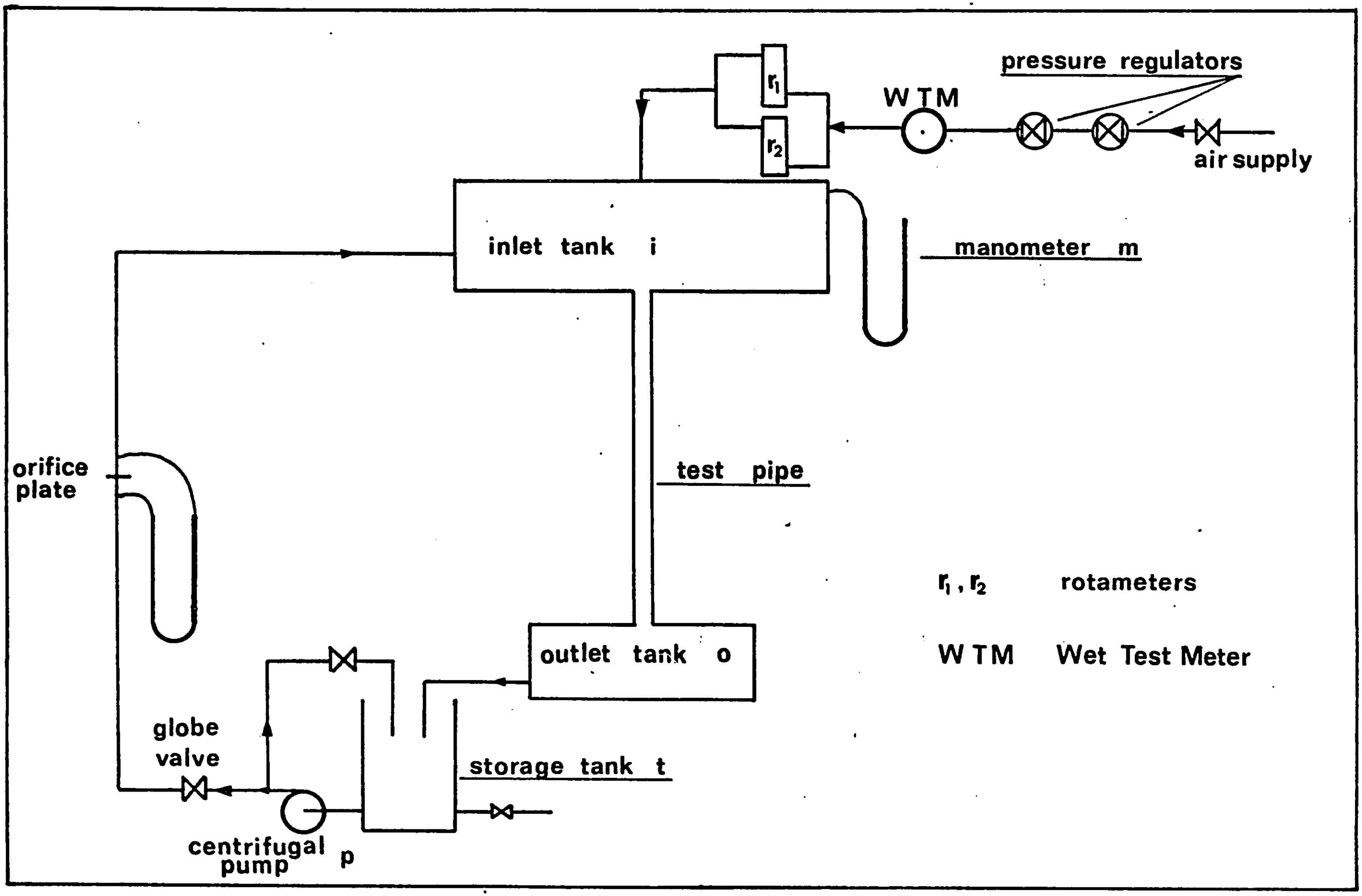

Figure 3·A Schematic Flow Diagram

DETAILS OF BAFFLES

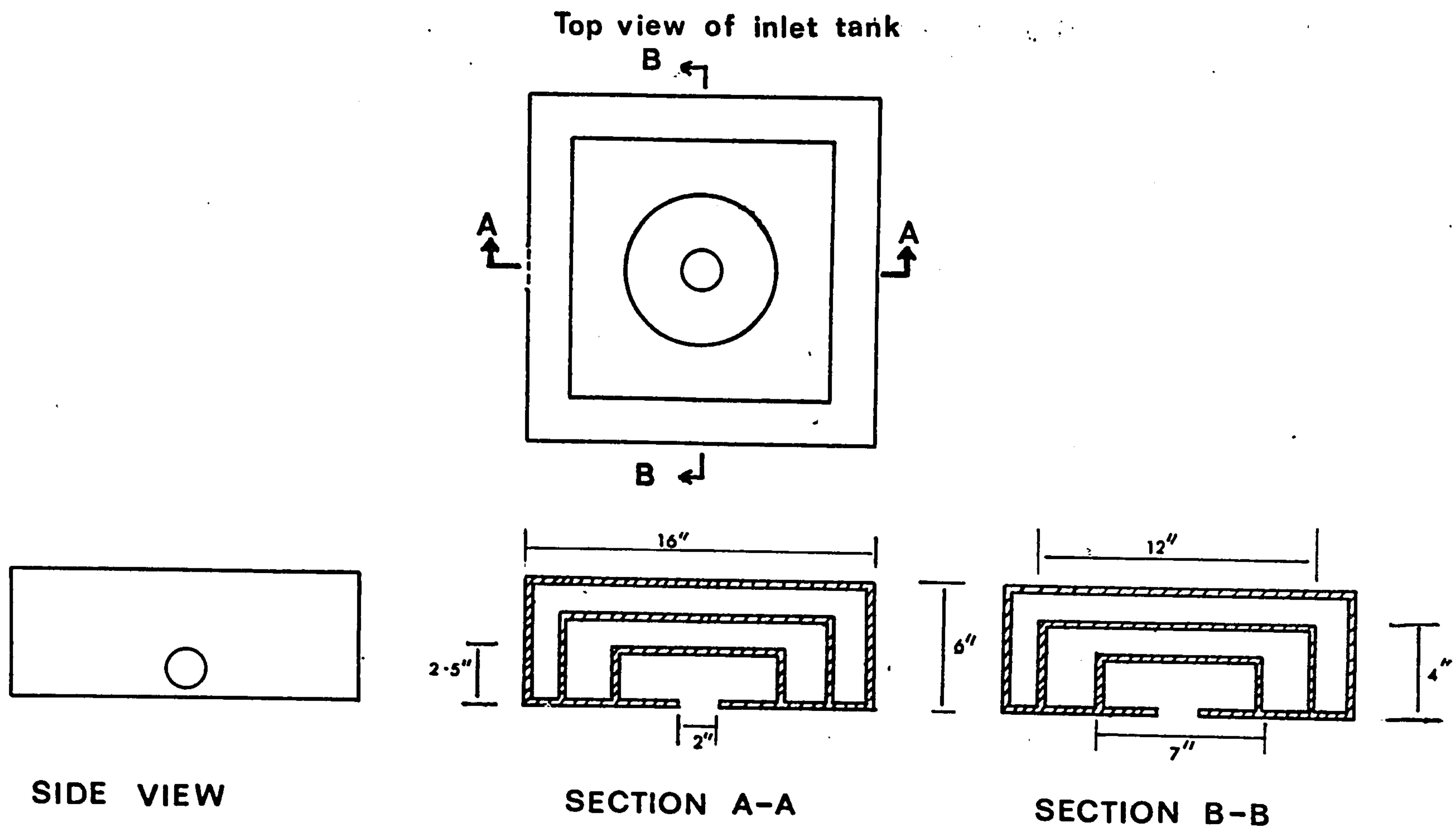

FIGURE 3·B

TABLE 3.1

Physical data for systems investigated

Pipe length = 12.0 ft.

Pipe diameters = 1.0, 1.5, 2.0 inches

Gas : Air

Density = 0.075 lb_m/ft^3

Viscosity = 0.018 centipoise

Physical properties of liquids

Liquid	Density (lb_m/ft^3)	Surface tension (dynes/cm)	Viscosity (cps)
Water	62.4	72.0	0.85
Sugar Solution 1	66.14	65.7	3.6
Sugar Solution 2	69.26	67.5	4.7

TABLES OF EXPERIMENTAL RESULTS

TABLES 3.2 - 3.10

TABLE 3.2

Liquid : Water

Pipe diameter : 1.0 inch

Liquid flow rate (ft^3/sec)	Air flow rate (ft^3/sec)
0.0050	0.00236
0.0066	0.0050
0.0090	0.00841
0.0115	0.00972
0.0135	0.0108
0.0150	0.0110
0.0165	0.0110
0.0190	0.0111
0.0210	0.0115
0.0223	0.0112
0.0287	0.0116

TABLE 3.3

Liquid : Water

Pipe diameter : 1.5 inches (0.125 ft)

Liquid flow rate (ft^3/sec)	Air flow rate (ft^3/sec)
0.00625	0.00533
0.00975	0.00929
0.01175	0.0100
0.0130	0.0106
0.0136	0.0105
0.0150	0.0110
0.0176	0.0107
0.0200	0.0108
0.0230	0.0107
0.0285	0.0108
0.0310	0.0108

TABLE 3.4

Liquid : Water

Pipe diameter : 2.0 inches

Liquid flow rate (ft^3/sec)	Air flow rate (ft^3/sec)
0.0075	0.00492
0.0095	0.00713
0.0122	0.00899
0.0140	0.0100
0.0150	0.0102
0.0200	0.0108
0.0250	0.0112
0.0285	0.0114
0.0310	0.0109
0.0340	0.0102
0.0370	0.00938

TABLE 3.

Liquid : Sugar Solution 1 (S1)

Pipe diameter : 1.0 inch

Liquid flow rate (ft^3/sec)	Air flow rate (ft^3/sec)
0.0080	0.00710
0.0095	0.00747
0.00975	0.00722
0.0120	0.00936
0.0140	0.0108
0.0142	0.0106
0.0153	0.0110
0.0173	0.0111
0.0185	0.0112
0.0197	0.0112

TABLE 3.6

Liquid : Sugar Solution 1

Pipe diameter : 1.5 inches

Liquid flow rate (ft^3/sec)	Air flow rate (ft^3/sec)
0.0060	0.0023
0.0085	0.0048
0.0103	0.0055
0.0140	0.0067
0.0158	0.0071
0.0173	0.0080
0.0180	0.0079
0.0198	0.0077
0.0210	0.0079
0.0275	0.0084
0.0300	0.0086

TABLE 3.7

Liquid : S1

Pipe diameter : 2.0 inches

Liquid flow rate (ft^3/sec)	Air flow rate (ft^3/sec)
0.0060	0.00
0.0098	0.0038
0.0108	0.0042
0.0143	0.0054
0.0173	0.0062
0.0210	0.0063
0.0275	0.0072
0.0295	0.0069

TABLE 3.8

Liquid : Sugar Solution 2 (S2)

Pipe diameter : 1.0 inch

Liquid flow rate (ft^3/sec)	Air flow rate (ft^3/sec)
0.0075	0.0060
0.0091	0.0074
0.00975	0.0083
0.0125	0.0100
0.0158	0.0109
0.0170	0.0110
0.0190	0.0113
0.0208	0.0111

TABLE 3.9

Liquid : S2

Pipe diameter : 1.5 inches

Liquid flow rate (ft^3/sec)	Air flow rate (ft^3/sec)
0.0103	0.0050
0.0123	0.0064
0.0130	0.0064
0.0173	0.0086
0.0188	0.0088
0.0195	0.0087
0.0207	0.0087
0.0243	0.0088
0.0263	0.0090

TABLE 3.10

Liquid : S2

Pipe diameter : 2.0 inches

Liquid flow rate (ft^3/sec)	Air flow rate (ft^3/sec)
0.0100	0.0041
0.0108	0.0050
0.0120	0.0062
0.0130	0.0071
0.0145	0.0085
0.0203	0.0099
0.0223	0.0100
0.0225	0.0100
0.0255	0.0103
0.0345	0.0093
0.0375	0.0086

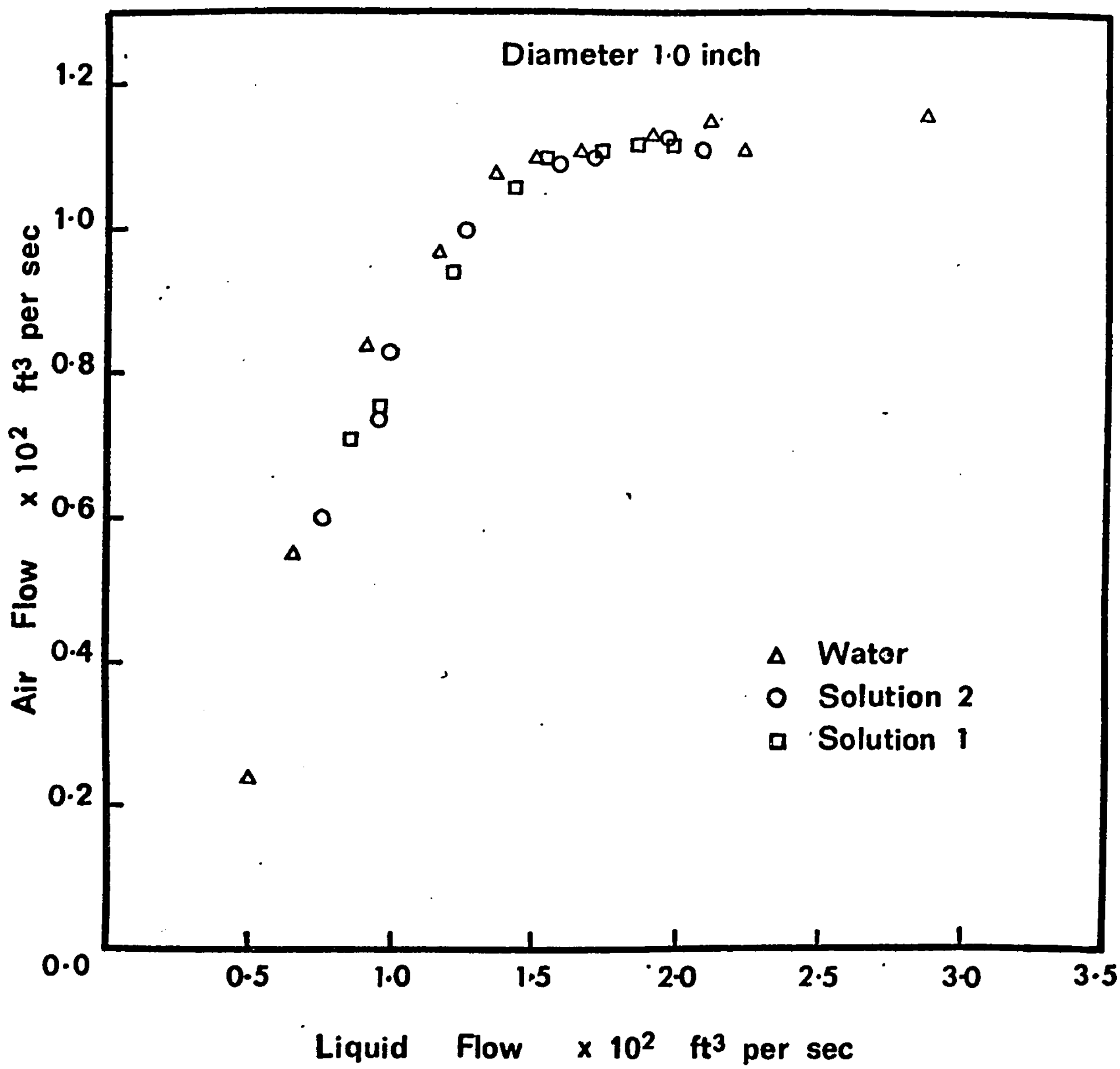
Diameter 1·0 inch
Air Flow x 10² ft³ per sec
Liquid Flow x 10² ft³ per sec
0·0
0·2
0·4
0·6
0·8
1·0
1·2
0·5
1·0
1·5
2·0
2·5
3·0
3·5
Water
Solution 2
Solution 1

Figure 3·1

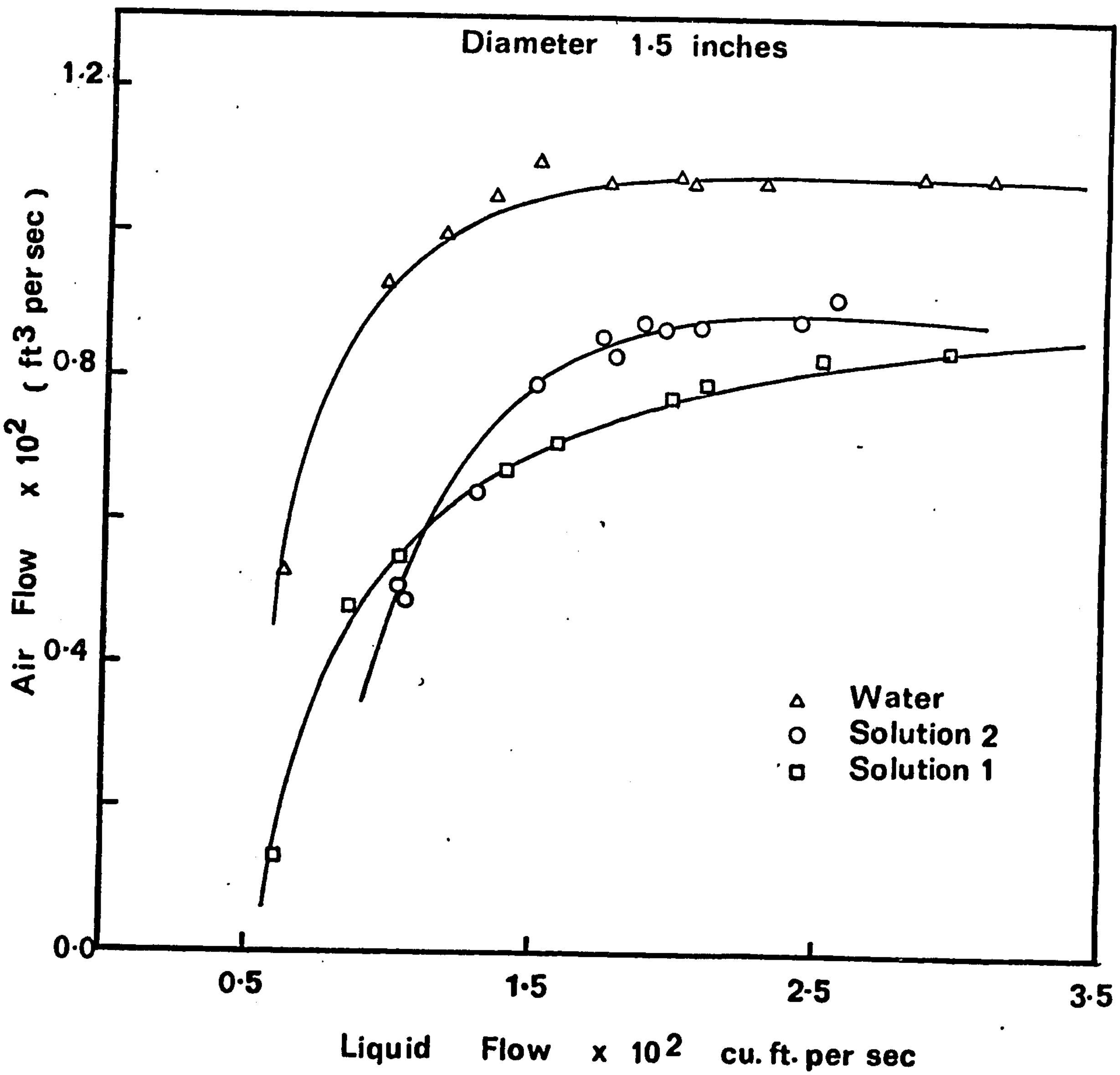
Diameter 1·5 inches
1·2
0·8
0·4
0·0
Air Flow x 10[2] (ft[3] per sec)
0·5
1·5
2·5
3·5
Liquid Flow x 10[2] cu. ft. per sec
Water
Solution 2
Solution 1

Figure 3·2

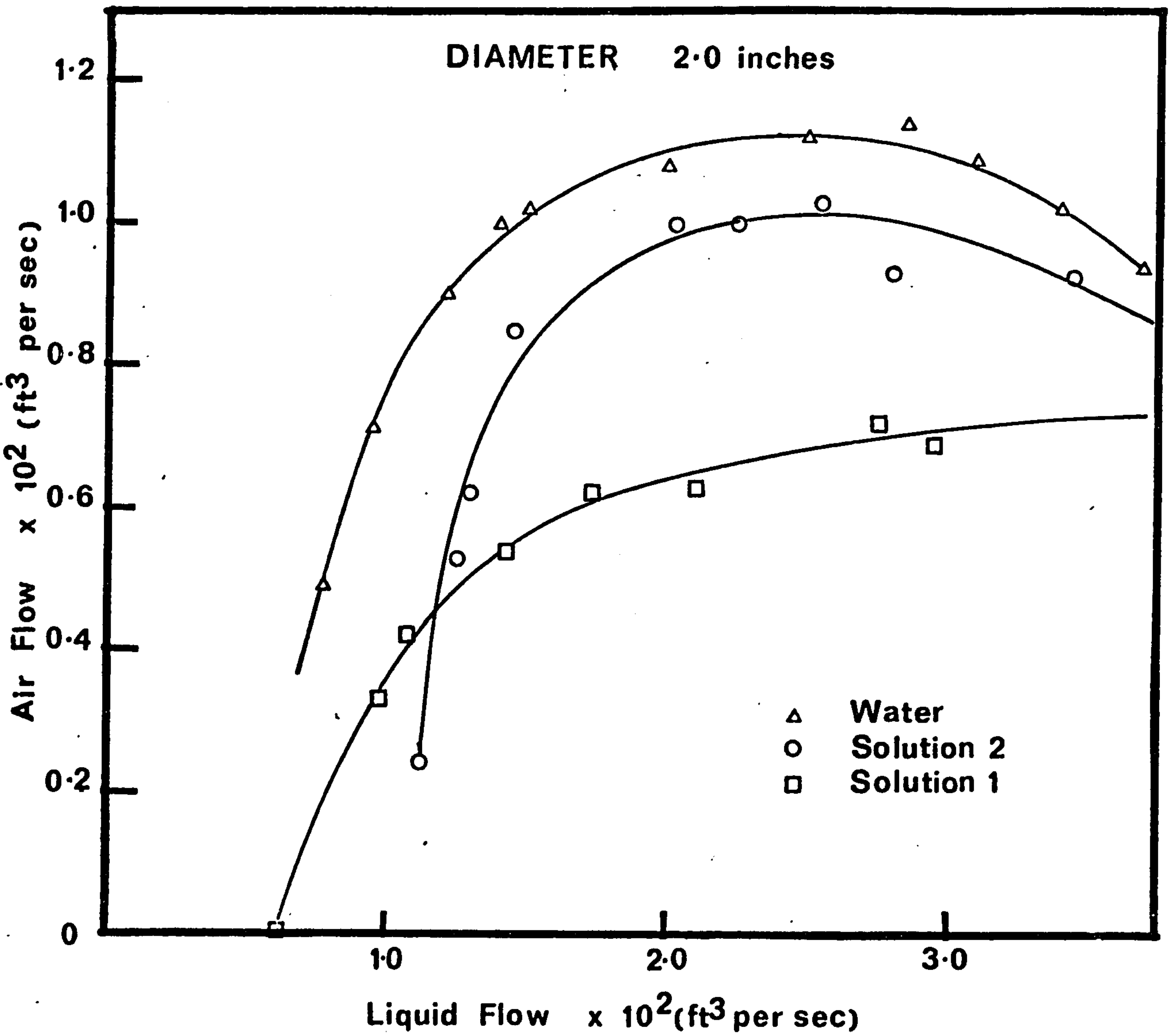

DIAMETER 2·0 inches
Water
Solution 2
Solution 1
Air Flow x 10^2 (ft^3 per sec)
Liquid Flow x 10^2(ft^3 per sec)
0
0·2
0·4
0·6
0·8
1·0
1·2
1·0
2·0
3·0

Figure 3·3

AIR – WATER DATA

DIAMETER: 1·0

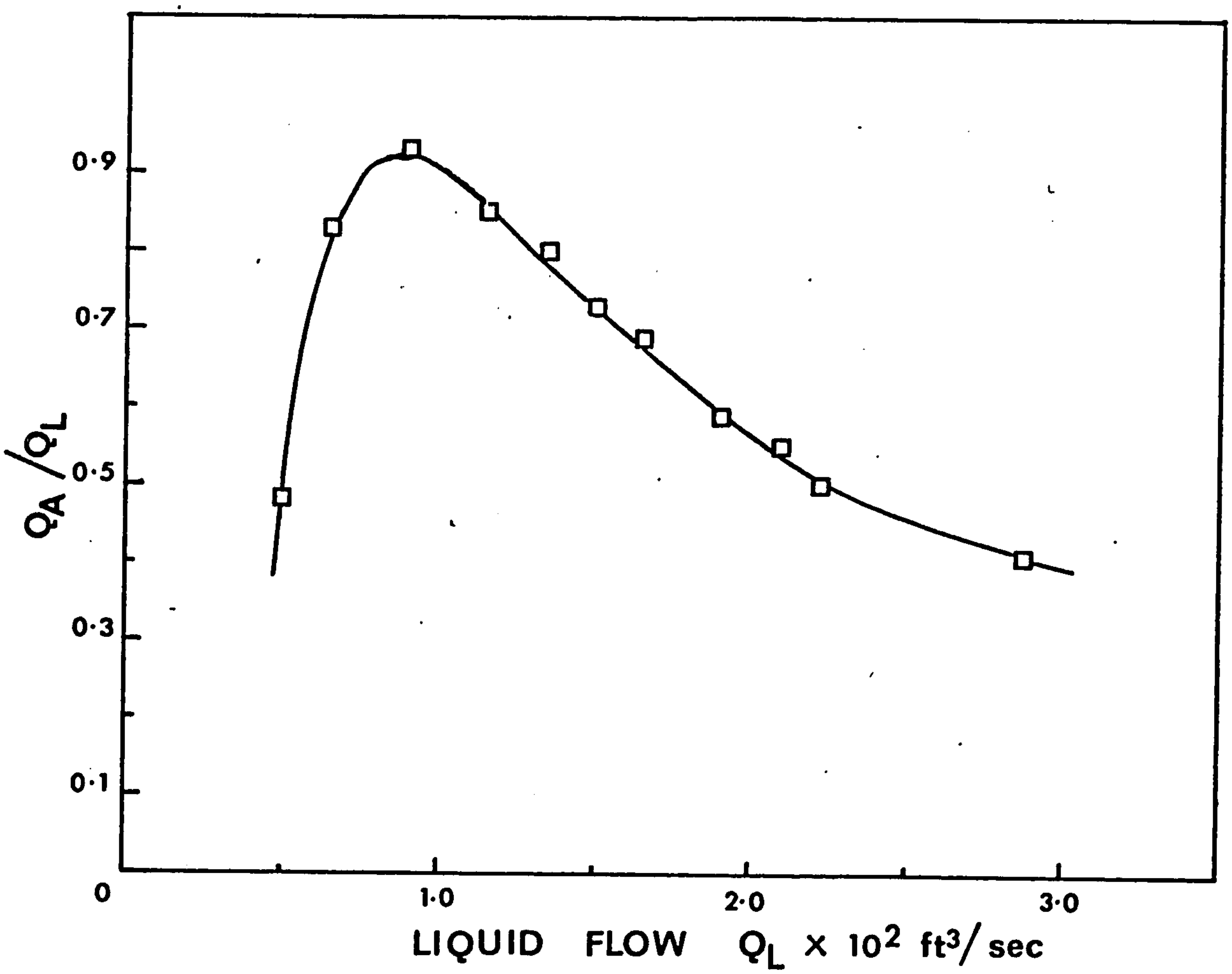

FIGURE 3·4

AIR - WATER DATA

DIAMETER: 1·5

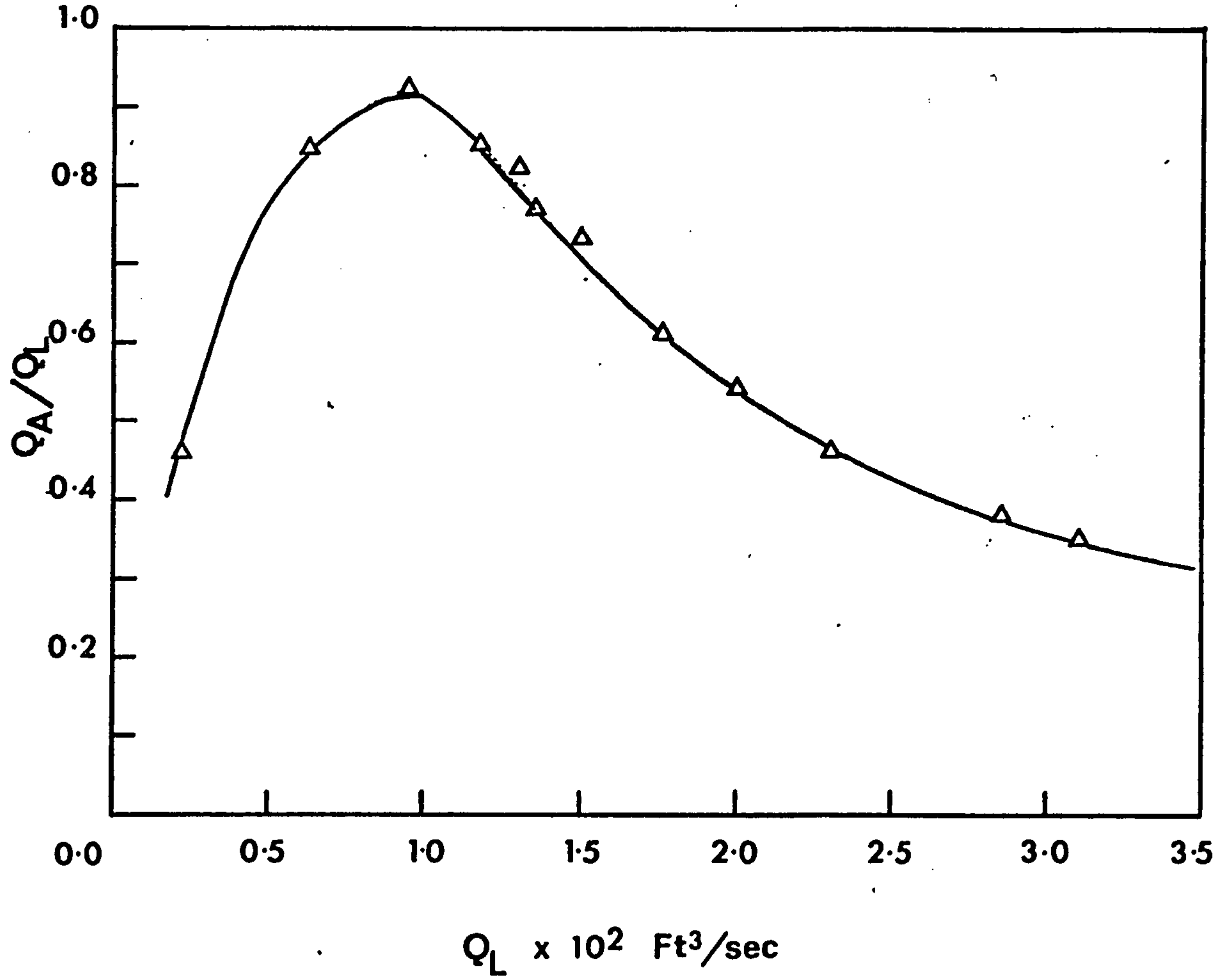

FIGURE 3·5

AIR – WATER DATA

DIAMETER : 2·0

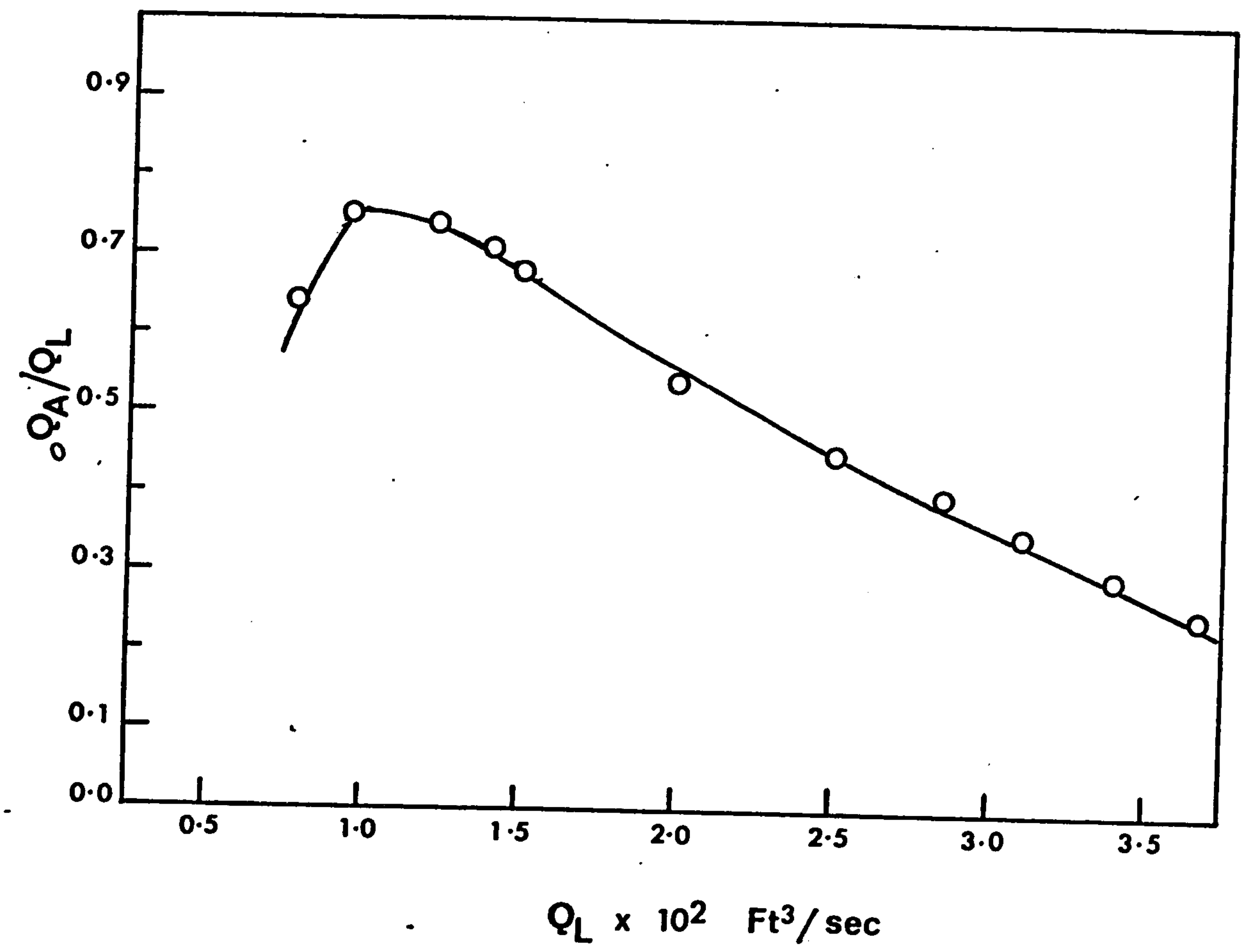

FIGURE 3·6

AIR - SOLUTION 1 DATA

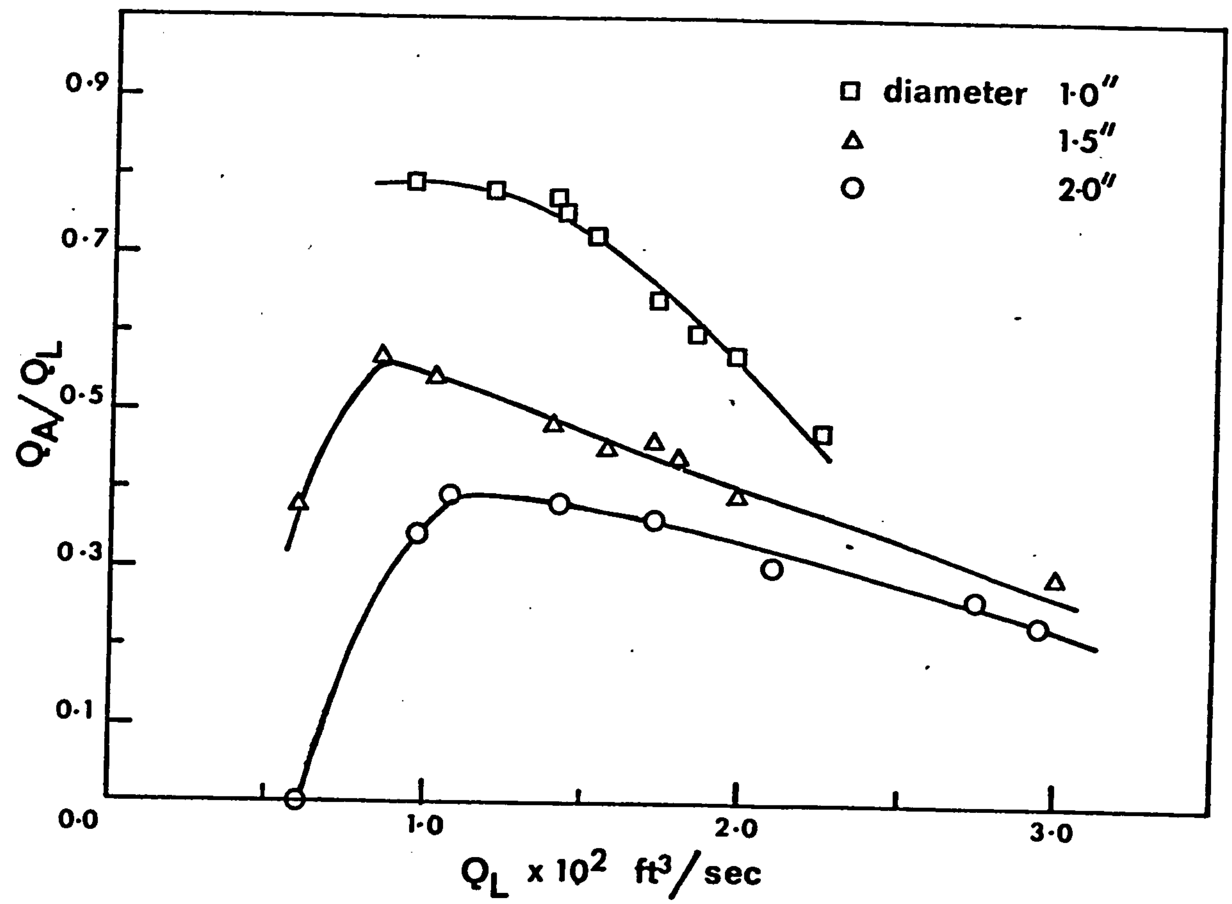

FIGURE 3·7

AIR – SOLUTION 2 DATA

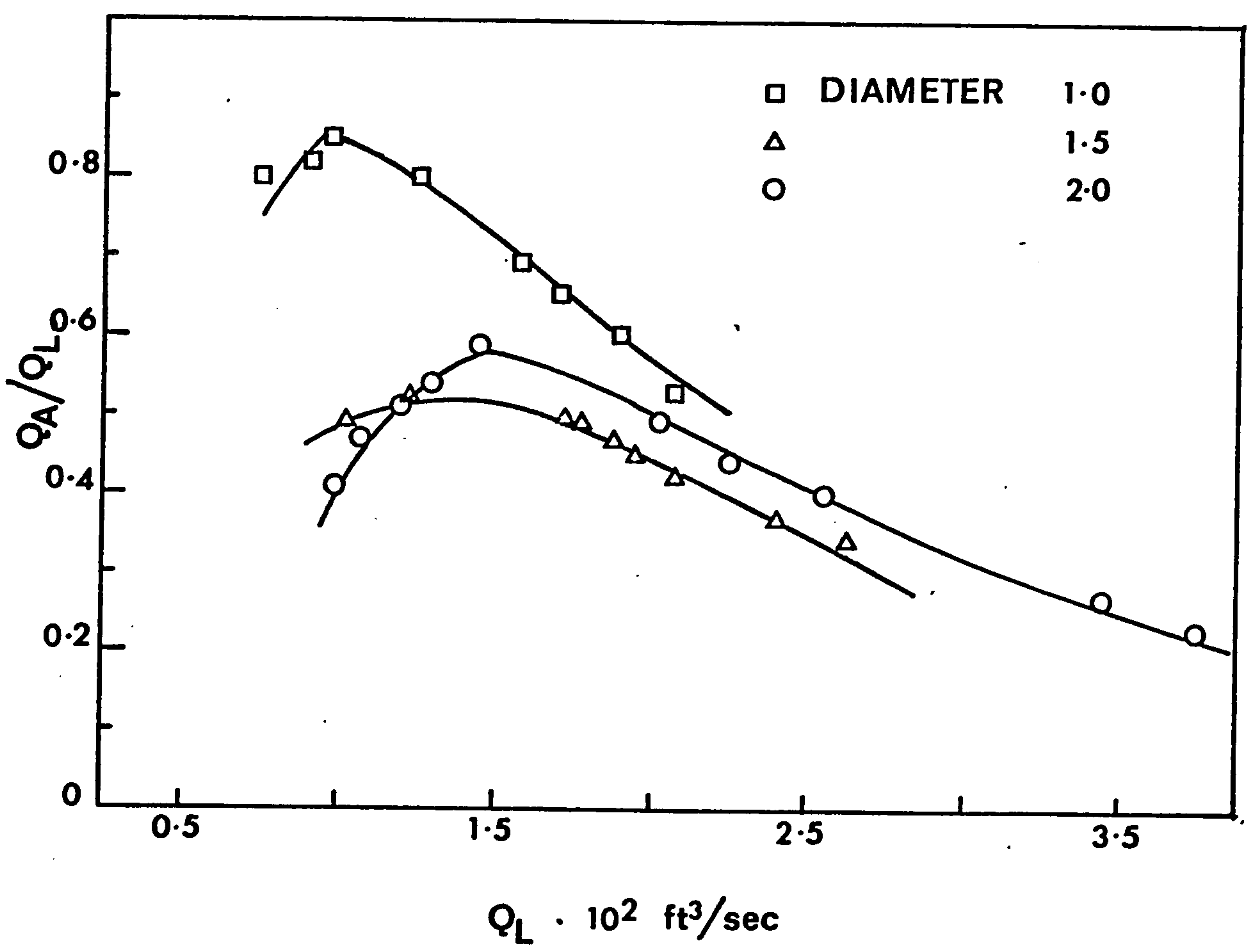

FIGURE 3·8

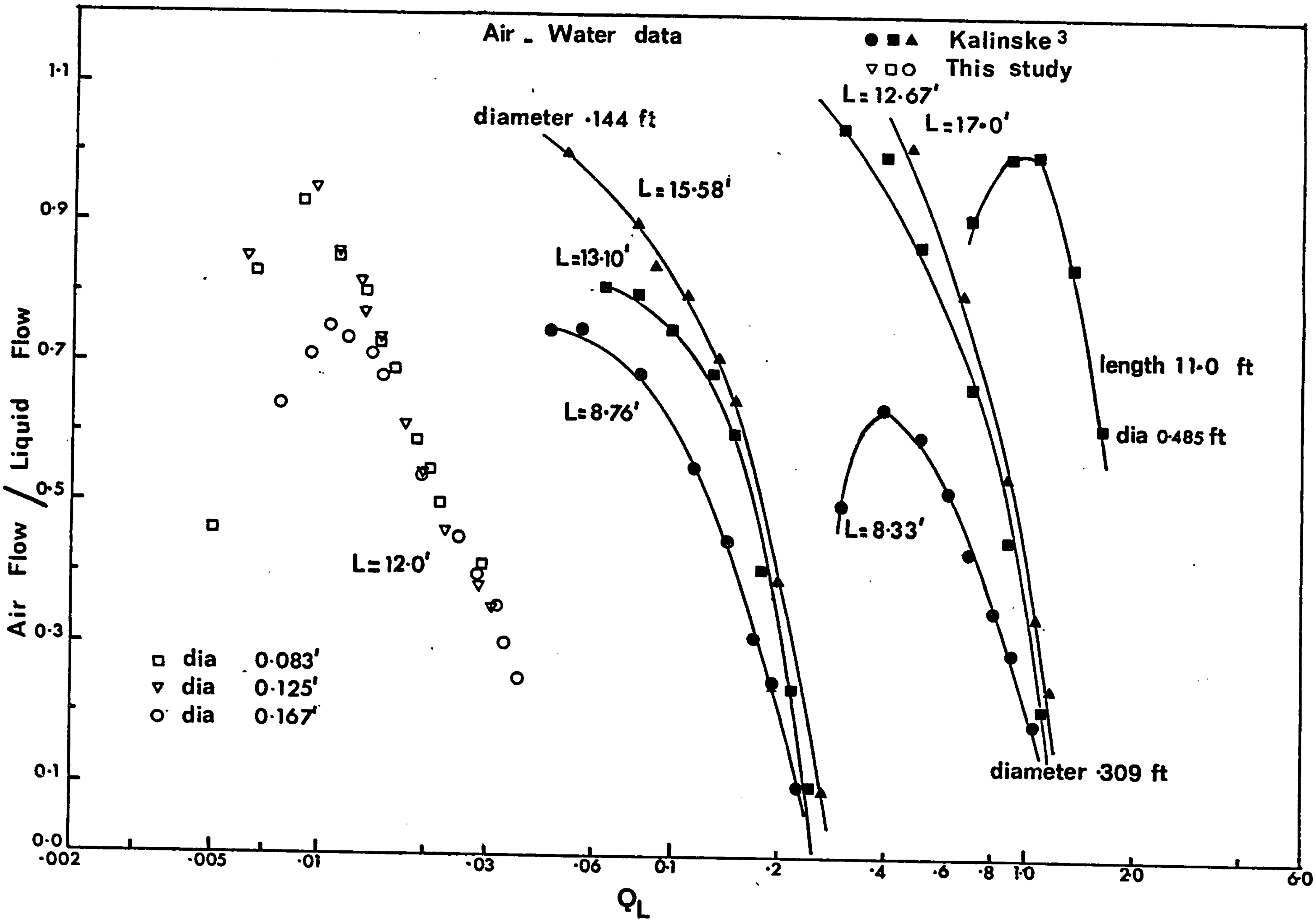

Air _ Water data
Kalinske 3
This study
diameter ·144 ft
L=15·58'
L=13·10'
L=8·76'
L=12·67'
L=17·0'
length 11·0 ft
dia 0·485 ft
L=8·33'
diameter ·309 ft
L=12·0'
dia 0·083'
dia 0·125'
dia 0·167'
Air Flow / Liquid Flow
Q_L

FIGURE 3·9

4 RESULTS AND DISCUSSION

The experimental results have been presented as graphs of air flow, Q_A , versus liquid flow, Q_L in Figures (3.1) - (3.3) and in the form Q_A / Q_L versus Q_L in Figures (3.4) - (3.8).

The graphs of Q_A vs Q_L show that, for a given size of pipe, there is a maximum amount of air which can be entrained, after which there is a decrease in air flow for increasing liquid flows. Theoretically, the air should decrease until it reaches zero when the pipe is flowing full of liquid. In this study, it was not possible to verify this experimentally because, at liquid flow rates in the range required to fill the pipes, the flow behaviour was so unsteady that any meaningful air flow measurements could not be taken.

At liquid flow rates in excess of those shown on the graphs, the following flow was observed.

(i) The tip of the vortex reached the mouth of the outlet pipe; and air was steadily entrained as indicated by the manometer on the inlet tank.

(ii) Suddenly, and without any change having been made in the liquid flow rate, the tip of the vortex no longer reached the mouth of the outlet pipe, but remained a short distance above it and air entrainment ceased.

(iii) Again without any change in liquid flow rate, the tip of the vortex necked down to the mouth of the outlet pipe and the whole sequence repeated itself.

The time taken for a complete cycle, steps (i - iii), varies, and air entrainment becomes a very unsteady process, as shown by the oscillation of the liquid levels in the manometer on the inlet tank. No actual measurements of either the length of cycle or air flow could be taken during this phenomenon.

This appearance, disappearance of the air core means that the height of liquid in the tank is now approaching the value h_c (as predicted by equations (2.5 - 2.7) and also indicates a transition from one flow regime to another in the pipe. The flow in the pipe at this time is no longer simple annular, and intermittent slugs of air travel down the pipe with the liquid. Air entrainment in this slug flow regime is now unsteady and, even though it was not actually measured, appears to be considerably reduced.

The onset of this unsteady process and, in general, the amount of air entrained seem to be a very strong function of the geometry of the flow system. This is suggested on the basis of a comparison between the experimental results of this study and the work of Kalinske, as shown in Figure (3.9). For example, by considering his experimental results for a pipe of length 13.1 feet and diameter 0.144 feet, it is seen that there was measurable air entrainment well in excess of the amount in this study, and at liquid flow rates much higher than those at which the unsteady process started in this study.

The graphs of Q_A / Q_L versus Q_L show that the maximum air-water ratio occurs at very low liquid flow rates which is in qualitative agreement with the work of Kalinske. Other similarities between the two studies were the formation of a weak vortex at the top of the test pipe and the existence of subatmospheric pressures in the inlet tank. As in Kalinske's experiments, the liquid flowed as a film along the pipe walls (up to certain liquid flow rates) with the air in the centre of the tube but, in contrast to his observations, the liquid was not filled with small air bubbles.

From Figure (3.9), it is observed that there are significant differences between the experimental results of Kalinske and this work. The basic principles and tecniques of flow measurements for the two studies were the same, but the dimensions and design of the experimental apparatus were different. Kalinske studied flow from a cylindrical tank of diameter 6 feet and height 2.5 feet, while the tank dimensions for this study were 16" x 16" x 6", the tank in each having been designed to eliminate swirl of the liquid in the tank. The observed difference between the two sets of experimental data could, therefore, be another indication of the unresolved difficulties involved in the scale up of air flow measurements taken in a model as previously discussed in References (7 - 9).

The graphs of air flow versus liquid flow indicate an apparent anomaly since, in each case, the results for the air - solution 2 system fall on a curve which lies between the curves for water and sugar solution 1. The values of β (as defined by equation (2.36)), or any group characterizing the physical properties considered here, do not follow such a pattern and no reasonable explanation for this apparent anomaly can be offered here.

On the basis of the groups developed in Sections (2.5.1) to (2.5.3), attempts were made to find an overall correlation scheme for the experimental results but no general correlating function was found. This means that, even if a liquid Reynolds number is specified, other parameters involving the pipe diameter and liquid properties are required to specify the air flow obtained. Graphs showing typical results for these attempts are shown in Figures (A.1) to (A.8).

By assuming that an equation involving three constants (equation 2.59) could represent the experimental results, it was possible to determine the values of the constants as shown in Table A.14. Considering that a multiple correlation coefficient of 1.0 indicates that all the experimental points fall on a curve given by equation (2.59), it is seen that equation (2.59) fits the experimental data reasonably well. The constants a, b, c in equation (2.59) do not follow any predictable pattern and no further general conclusions can be drawn from these results at this time.

In Figure A.1, graphs of the Froude number for the air have been plotted against the liquid Reynolds number, to show the comparison between the results for the air-water system and the air-solution 2 system. For each liquid system, a different family of curves is obtained, where the data for each pipe diameter falls on a separate curve.

In Figures (A.2 - A.4), graphs of the Reynolds number of the air (based on total pipe cross sectional area) have been plotted against the liquid Reynolds number to show the comparison between the results for the various liquids. Again a family of curves is obtained for different pipe diameters in the same air-liquid system. For any liquid system, the curves may be considered to have β as a parameter, but the difference in the curves for water and any of the sugar solutions is not completely represented in terms of β alone. The results for the two sugar solutions show that (except for solution 2 flowing in a 2 inch diameter pipe) all the experimental data may be represented by a plot of Re_{AT} versus Re_L with β as a parameter. The differences in physical properties of the sugar solutions (as represented by K_F in Table 2.2) are smaller than the differences between water and any sugar solution. This could be the reason for the lateral spread in the curves for water and the sugar solutions.

In Figures (A.5) and (A.6), Re_A has been plotted against Re_L. These plots do not lead to any more general correlation than do Figures (A.2 - A.4), and the comments concerning Figures (A.2) to (A.4) are equally relevant. In Figures (A.7) and (A.8), typical plots of Re_A and $(V_A / V_1)^2$ versus Re_L have been presented.

5 CONCLUSIONS

The main objective of this study was to investigate whether or not the amount of air entrained by a flowing liquid could be adequately represented by simple dimensionless groups involving the properties of the system. The attempts at correlation have been discussed in previous sections and show that, at the present, it will not be possible to predict the amount of air entrained, using any of the methods outlined in this thesis. Other evidence, concerning the extreme difficulty in predicting the amount of air entrained by a liquid, has been presented in Reference (9). This paper, which was published after the experimental work for this thesis had already been started, discussed the work of investigators at the Hydraulic Research Station, Wallingford. These investigators, in an attempt to relate air entrainment to model scale, tested models of air entraining structures to scales 1:10, 1:20, 1:30 without any general result. The failure to obtain a general correlation by the methods of Section 2.5 should not, therefore, be surprising.

The phenomenon of vapour entrainment must be due to the transfer of momentum from the liquid to the air as the liquid flows into the top of the tube. A complete analysis of such flow is not possible in this study. The flow in the inlet region of the pipe might be strongly influenced by the details of each individual system. This is observed in the difference between the experimental results of Kalinske and this work.

Suggestions for future work.

In this study, the amount of air entrained was measured by supplying air to the inlet tank to maintain atmospheric pressure in the tank. Such a method could not allow for the measurement of any pressure drops in the entrance region of the inlet pipe. By using a different method of measuring the air entrained, future work could include

(i) measurement of pressure gradients over the length of the tube, and

(ii) measurement of size of air core at various points in the tube.

The theoretical analysis presented in the Appendix to Dukler's work(26) might be modified to provide other parameters for describing the flow.

NOMENCLATURE

Symbol	Meaning
a,b,c	constants in empirical correlation (eq. 2.59)
C_i	entrance loss coefficient (eq. 2.9)
C_o	exit loss coefficient (eq. 2.10)
d_a	diameter of air core
D	pipe diameter
E_m	efficiency of momentum transfer (eq. 2.54)
f	friction factor
g	gravitational acceleration
g_c	gravitational constant $(lb_m / lb_f)(ft\ sec^{-2})$
h_c	head of liquid at which pipe flows full (eq. 2.13)
h_o	head at which air entrainment starts (eq. 2.5)
k_1, k_2	constants (eq. 2.56)
L	pipe length
m	thickness of liquid film
M_A	momentum of air (eq. 2.51)
M_I	ideal momentum transferred to air (eq. 2.53)
P	pressure
Q_A	air flow (cu. ft. per sec.)
Q_{Am}	maximum air flow (eq. 1.2)

Q_L	liquid flow (cu. ft. per sec.)
Q_{LF}	flow rate at which pipe flows full of liquid
r	radial co-ordinate
r_i	radius of air core
R	pipe radius
u	velocity in axial direction
u^+	dimensionless velocity component
u^*	friction velocity
v	average velocity
V_A	an average velocity of air (eq. 2.47)
V_{AT}	an average velocity of air (eq. 2.42)
V_i	interface velocity of liquid
V_{LT}	mean linear velocity of liquid
V_L	superficial linear liquid velocity
V_m	maximum liquid velocity (eq. 1.1)
y	distance in liquid film from pipe wall
y_i	distance from pipe wall to surface of liquid fil
y^+	dimensionless distance parameter (eq. 2.20)
Y	dimensionless value of y^+ at interface
V_c	critical liquid velocity (eq. 2.2)

Dimensionless groups

Fr_A	Froude number of air (eq. 2.46)
Fr_{AT}	Froude number of air (eq. 2.43)
Re_{AT}	Reynolds number of air (eq. 2.44)
Re_A	Reynolds number of air (eq. 2.45)
Re_L	Reynolds number of liquid (eq. 2.39)
Re_F	Reynolds number at which pipe flows full of liquid (eq. 2.15)
Re_I	interfacial Reynolds number of liquid (eq. 2.55)
K_F	Film number (eq. 2.41)

Greek symbols

β	dimensionless number (eq. 2.36)
ρ_A	density of air
ρ_L	density of liquid
μ_A	viscosity of air
μ_L	viscosity of liquid
σ_L	surface tension of liquid
ϕ_1, ϕ_2	function definitions (eq. 2.45, 2.46)
τ_w	shear stress at pipe wall
ϕ_3, ϕ_4	function definitions (eq. 2.49, 2.50)

REFERENCES

1. Gouse, An index to two phase gas-liquid flow literature. M.I.T., Report No. 9, M.I.T. Press.

2. Peele, R., Compressed air plants, Wiley, 1930.

3. Sourour, S., M. Eng. Thesis 1970, McGill University.

4. Dawson, F. and Kalinske, A., Report on hydraulics and pneumatics of plumbing drainage systems. University of Iowa Studies in Engineering, Bulletin No. 10, 1937.

5. Kalinske, A. A., Hydraulics of drain and overflow pipes. University of Iowa Studies in Engineering, Bulletin No. 26, 1939.

6. Laushey, L. M. and Mavis, F. T., Air entrainment by water flowing down vertical shafts. Proceedings International Association for Hydraulic Research, 1953.

7. Hall, L. S., Trans. Amer. Soc. Civ. Engrs., 109, (1945), 150.

8. Peterka, A. J., Trans. Amer. Soc. Civ. Engrs., 121, (1956), 385.

9. Binnie, A. M. and Simms, G. P., Air entrainment by flowing water under reduced atmospheric pressure, Journal of Hydraulic Research, Vol. 7, No. 3, 1969.

10. Williamson, J., Proc. Inst. Civ. Engrs., 231, (1931), 275.

11. Naylor, A. H., Siphon Spillways (p.26) London, Arnold 1935.

12. Binnie, A. M., Proc. Roy. Soc. London, 168-A, 219 (1938).

13. Anwar, H. O., Coefficients of discharge for gravity flow into vertical pipes. Journal of Hydraulic Research, No.1, vol. 3, 1965.

14. Harleman, D.F., Purple, R., Morgan, R., International

Association for Hydraulic Research, 8th congress, August 1959.

15. Lubin, B. T. and Springer, G. S., J. Fluid Mech., 29, 385 (1967).

16. Gluck, J. et al., J. Spacecraft, Vol. 3, No. 11 (1966).

17. Drew, T. B. et al., Trans. Amer. Inst. Chem. Engrs., 28, 56 (1932).

18. Haindl, K., Contribution to air entrainment by a vortex. International Association for Hydraulic Research, 8th Congress, August 1959.

19. Anwar, H. O., Formation of a weak vortex. Journal of Hydraulic Research, No. 1, Vol. 4 (1966).

20. Von Karman, T., Trans. Amer. Soc. Mech. Engrs., 61, 705 (193

21. Nikuradse, J., Forchungsheft, 361, 1 (1933).

22. Dukler, A. and Bergelin, P., Chem. Eng. Prog., 48, 557 (1952

23. Anderson, G. and Mantzouranis, B., Chem. Eng. Sci., Vol. 12 (1960).

24. Levy, S., Int. Jour. of Heat Transfer, Vol. 9 (1966).

25. Catchpole, J. and Fulford, G., Ind. and Eng. Chem., Vol. 58, No. 3 (1966).

26. Dukler, A. E., Chem. Eng. Progr. Symp. Ser., Vol. 56, No. 30 (1960).

27. Deissler, R. G., Unsteady viscous vortex with flow toward the centre. J. Appl. Sci. Res., Vol. 16, No. 1, 1966.

28. Dergarabedian, P., The behaviour of vortex motion in an emptying container. Proc. Heat Transfer and Fluid Mech. Inst., 1960.

29. Toyokura, T. and Akaike, S., Bulletin JSME, Vol. 13, No. 57, 1970.

30. Granger, R., Jour. Fluid Mech., Vol. 25 (1966).

31. ASME Power Test Code 1959, Supplement on Instruments and Apparatus Part 5, Chapter 4, Flow measurement.

APPENDIX

TABLE A.1

Comparison between equations (1.1) and (1.2) and experimental results.

Pipe diameter : 1.0 inch

Q_L (ft^3 /sec) measured	Q_A (ft^3/sec) measured	Q_A / Q_{Am} equations (1.1), (1.2)
0.0050	0.0024	- 2.82
0.0066	0.0050	- 2.55
0.0090	0.0084	- 2.24
0.0115	0.0097	- 1.70
0.0135	0.0108	- 1.47
0.0150	0.0110	- 1.28
0.0165	0.0110	- 1.12
0.0190	0.0111	- 0.93
0.0210	0.0115	- 0.84
0.0223	0.0112	- 0.57

TABLE A.2

Pipe diameter : 1.5 inches

Q_L (ft^3/sec) measured	Q_A (ft^3/sec) measured	Q_A / Q_{Am} equations (1.1),(1.2)
0.0062	0.0053	0.91
0.0097	0.0093	1.96
0.0117	0.0100	2.60
0.0130	0.0106	3.27
0.0136	0.0105	3.57
0.0150	0.0110	5.00
0.0176	0.0107	14.51
0.0200	0.0108	- 15.42
0.0230	0.0107	- 4.13
0.0285	0.0108	- 1.72
0.0310	0.0108	- 1.35

TABLE A.3

Pipe diameter : 2.0 inches

Q_L (ft^3/sec) measured	Q_A (ft^3/sec) measured	Q_A / Q_{Am} equations (1.1), (1.2)
0.0077	0.0049	0.26
0.0095	0.0071	0.37
0.0122	0.0090	0.46
0.0140	0.0100	0.51
0.0150	0.0102	0.52
0.0200	0.0108	0.58
0.0250	0.0112	0.65
0.0285	0.0114	0.71
0.0310	0.0109	0.72
0.0340	0.0102	0.74
0.0370	0.0094	0.75

TABLE A.4

Liquid : Water

Pipe diameter : 1.0 inch

Q_{LF} : 0.071 ft^3/sec

Q_A/Q_L	Re_L/Re_F	Re_{AT}	Fr_{AT}	Re_A	$Re_L \times 10^{-3}$	$Re_I \times 10^{-4}$	V_i (ft/sec)	$2(V_A/V_i)^2$	d_a (ft)
0.46	0.007	224	0.022	247	8.35	5.72	6.28	0.07	0.075
0.83	0.009	474	0.047	534	11.0	6.47	7.11	0.27	0.074
0.93	0.127	796	0.079	923	15.0	7.30	8.02	0.66	0.072
0.85	0.162	921	0.091	1090	19.2	8.04	8.83	0.80	0.070
0.80	0.190	1020	0.101	1240	22.5	8.54	9.38	0.95	0.069
0.73	0.211	1040	0.103	1280	25.0	8.88	9.75	0.96	0.068
0.69	0.232	1040	0.103	1300	27.5	9.23	10.14	0.94	0.067
0.59	0.268	1050	0.104	1340	31.7	9.79	10.76	0.95	0.065
0.55	0.296	1090	0.107	1420	35.1	10.10	11.14	1.01	0.064
0.50	0.313	1060	0.105	1400	37.2	10.40	11.40	0.96	0.063
0.41	0.404	1100	0.108	1540	47.9	11.50	12.64	1.08	0.060

TABLE A.5

Liquid : Water

Pipe diameter : 1.5 inches

Q_{LF} : 0.195 ft^3/sec

Q_A/Q_L	Re_L/Re_F	Re_{AT}	Fr_{AT}	Re_A	Re_L x 10^{-3}	Re_I x 10^{-4}	V_i (ft/sec)	$2(V_A/V_i)^2$	d_a (ft)
0.853	0.032	337	0.022	356	6.95	7.86	5.75	0.071	0.118
0.953	0.050	587	0.039	633	10.8	9.55	6.99	0.157	0.116
0.853	0.060	631	0.042	686	13.1	10.2	7.44	0.165	0.115
0.815	0.067	669	0.044	731	14.5	10.5	7.69	0.177	0.115
0.769	0.070	663	0.043	725	15.1	10.6	7.75	0.172	0.114
0.732	0.077	694	0.046	765	16.7	11.2	8.17	0.175	0.114
0.608	0.090	676	0.044	754	19.6	12.1	8.86	0.148	0.112
0.541	0.103	682	0.045	767	22.3	12.6	9.25	0.143	0.111
0.464	0.118	676	0.044	768	25.6	13.3	9.73	0.132	0.110
0.379	0.146	6.82	0.045	790	31.7	14.5	10.59	0.123	0.108

TABLE A.6

Liquid : Water

Pipe diameter : 2.0 inches

Q_{LF} : 0.375 ft^3/sec

Q_A/Q_L	Re_L/Re_F	Re_{AT}	Fr_{AT}	Re_A	Re_L x 10^{-3}	Re_I x 10^{-4}	V_i (ft/sec)	$2(V_A/V_i)^2$	d_a (ft)
0.635	0.021	233	0.012	243	6.47	10.3	5.65	0.019	0.160
0.750	0.025	338	0.017	354	7.93	11.2	6.14	0.034	0.159
0.736	0.032	426	0.021	449	10.2	12.4	6.79	0.045	0.158
0.714	0.037	474	0.023	501	11.7	12.8	7.05	0.052	0.158
0.679	0.040	483	0.024	512	12.5	13.2	7.23	0.052	0.157
0.541	0.053	511	0.025	550	16.7	15.1	8.31	0.047	0.155
0.451	0.067	530	0.026	576	20.9	16.5	9.08	0.044	0.153
0.401	0.076	540	0.027	590	23.8	17.2	9.45	0.043	0.153
0.352	0.083	516	0.025	567	25.9	17.9	9.82	0.037	0.152
0.300	0.091	483	0.024	534	28.4	18.5	10.17	0.031	0.151
0.253	0.099	444	0.022	494	30.9	19.1	10.51	0.025	0.150

TABLE A.7

Liquid : Sugar Solution 1 (S1)

Pipe diameter : 1.0 inch

Q_{LF} : 0.068 ft^3/sec

Q_A/Q_L	Re_L/Re_F	Re_{AT}	Fr_{AT}	Re_A	Re_L 10^{-3}	$Re_I \times 10^{-4}$	V_i (ft/sec)	$2(V_A/V_i)^2$	d_a (ft)
0.84	0.118	672	0.066	791	3.34	1.60	7.01	0.65	0.071
0.79	0.140	707	0.070	847	3.97	1.70	7.48	0.68	0.070
0.74	0.143	684	0.067	820	4.07	1.71	7.51	0.63	0.070
0.78	0.176	886	0.087	1090	5.01	1.84	8.07	1.01	0.068
0.77	0.206	1020	0.101	1290	5.85	1.97	8.64	1.30	0.066
0.75	0.209	1000	0.099	1270	5.93	1.98	8.69	1.25	0.066
0.72	0.224	1040	0.103	1330	6.39	2.03	8.91	1.33	0.065
0.64	0.254	1050	0.104	1370	7.23	2,15	9.43	1.34	0.064
0.60	0.272	1060	0.105	1400	7.73	2.21	9.68	1.37	0.063
0.57	0.290	1060	0.105	1420	8.23	2.26	9.93	1.37	0.062

TABLE A.8

Liquid : S1

Pipe diameter : 1.5 inches

Q_{LF} : 0.178 ft^3/sec

Q_A/Q_L	Re_L/Re_F	Re_{AT}	Fr_{AT}	Re_A	$Re_L \times 10^{-3}$	$Re_I \times 10^{-4}$	V_i (ft/sec)	$^2(V_A/V_i)^2$	d_a (ft)
0.38	0.034	145	0.0095	155	1.67	1.79	5.23	0.017	0.117
0.57	0.048	303	0.020	329	2.37	2.08	6.08	0.057	0.115
0.54	0.058	347	0.023	381	2.87	2.24	6.56	0.067	0.114
0.48	0.079	423	0.028	472	3.90	2.48	7.27	0.086	0.112
0.45	0.085	448	0.029	504	4.40	2.60	7.61	0.091	0.111
0.46	0.097	505	0.033	571	4.82	2.70	7.89	0.110	0.111
0.44	0.101	499	0.033	567	5.01	2.76	8.08	0.105	0.110
0.39	0.111	486	0.032	556	5.51	2.85	8.35	0.096	0.109
0.38	0.118	499	0.033	573	5.85	2.92	8.53	0.098	0.109
0.32	0.154	530	0.035	628	7.66	3.28	9.60	0.099	0.106
0.29	0.168	543	0.036	648	8.35	3.38	9.88	0.101	0.105

TABLE A.9

Liquid : S1

Pipe diameter : 2.0 inches

Q_{LF} : 0.35 ft^3/sec

Q_A/Q_L	Re_L/Re_F	Re_{AT}	Fr_{AT}	Re_A	$Re_L \times 10^{-3}$	$Re_I \times 10^{-4}$	V_i	$2(V_A/V_i)^2$	d_a
0.0	0.017	0.0	0.0	0.0	1.25	2.05	4.50	0.0	0.160
0.34	0.028	180	0.0089	190	2.05	2.47	5.43	0.013	0.158
0.39	0.031	199	0.0098	211	2.26	2.72	5.97	0.013	0.157
0.44	0.041	256	0.0126	274	2.99	3.05	6.69	0.018	0.155
0.36	0.049	294	0.0145	317	3.61	3.27	7.17	0.021	0.154
0.30	0.060	298	0.0147	325	4.39	3.48	7.64	0.020	0.153
0.26	0.079	341	0.0168	377	5.74	3.86	8.46	0.022	0.151
0.23	0.084	327	0.0161	363	6.16	3.99	8.77	0.20	0.150

TABLE A. 10

Liquid : S2

Pipe diameter : 1.0 inch

Q_{LF} : 0.065 ft^3/sec

Q_A/Q_L	Re_L/Re_F	Re_{AT}	Fr_{AT}	Re_A	Re_L $\times 10^{-3}$	Re_I $\times 10^{-4}$	V_i	$2(V_A/V_i)^2$	d_a
0.80	0.115	568	0.056	667	2.51	1.23	6.71	0.50	0.071
0.82	0.140	701	0.069	839	3.05	1.32	7.23	0.72	0.070
0.85	0.150	786	0.077	947	3.27	1.35	7.38	0.88	0.069
0.80	0.192	947	0.093	1180	4.19	1.50	8.23	1.20	0.067
0.69	0.243	1030	0.102	1330	5.29	1.63	8.91	1.38	0.065
0.65	0.262	1040	0.103	1370	5.70	1.68	9.19	1.40	0.064
0.60	0.292	1070	0.105	1440	6.37	1.76	9.62	1.48	0.062
0.53	0.320	1050	0.104	1440	6.97	1.82	9.98	1.45	0.061

TABLE A.11

Liquid : S2

Pipe diameter : 1.5 inches

Q_{LF} : 0.177 ft^3/sec

Q_A/Q_L	Re_L/Re_F	Re_{AT}	Fr_{AT}	Re_A	$Re_L \times 10^{-3}$	$Re_I \times 10^{-4}$	V_i	$2(V_A/V_i)^2$	d_a
0.49	0.058	316	0.021	348	2.30	1.78	6.48	0.057	0.114
0.52	0.069	404	0.027	449	2.75	1.90	6.93	0.086	0.112
0.49	0.073	404	0.027	451	2.90	1.95	7.12	0.083	0.112
0.50	0.097	543	0.036	617	3.86	2.14	7.82	0.132	0.110
0.47	0.106	556	0.037	635	4.20	2.20	8.04	0.134	0.109
0.45	0.110	549	0.036	631	4.36	2.26	8.26	0.127	0.109
0.42	0.117	549	0.036	635	4.62	2.32	8.47	0.123	0.108
0.36	0.137	556	0.037	654	5.43	2.49	9.10	0.117	0.106
0.34	0.148	568	0.037	672	5.87	2.55	9.30	0.120	0.106

TABLE A.12

Liquid : S2

Pipe diameter : 2.0 inches

Q_{LF} : 0.345 ft^3/sec

Q_A/Q_L	Re_L/Re_F	Re_{AT}	Fr_{AT}	Re_A	Re_L x 10^{-3}	Re_I x 10^{-4}	V_i	$2(V_A/V_i)^2$	d_a
0.41	0.029	194	0.0096	205	1.68	2.02	5.53	0.014	0.158
0.47	0.031	237	0.012	252	1.81	2.13	5.82	0.020	0.157
0.51	0.035	294	0.015	313	2.01	2.23	6.11	0.028	0.156
0.54	0.038	336	0.017	360	2.18	2.29	6.25	0.035	0.156
0.59	0.042	402	0.020	433	2.43	2.41	6.60	0.046	0.155
0.49	0.059	469	0.023	511	3.40	2.72	7.45	0.052	0.153
0.45	0.065	474	0.023	518	3.74	2.79	7.64	0.051	0.152
0.44	0.065	474	0.023	519	3.77	2.81	7.70	0.050	0.152
0.40	0.074	480	0.024	539	4.27	2.99	8.19	0.049	0.151
0.27	0.100	440	0.022	495	5.78	3.31	9.06	0.035	0.148
0.23	0.109	407	0.020	460	6.28	3.42	9.34	0.029	0.148

TABLE A.13

Typical results for equation (2.56)

Air-Water data

Pipe diameter : 2.0 inches

Re_A / Re_L calculated eq.(2.56)	Re_A / Re_L experimental
9.95	0.038
9.61	0.045
8.65	0.044
6.83	0.043
6.08	0.041
4.62	0.033
- 2.77	0.025
- 4.41	0.022
- 7.12	0.019
- 9.79	0.016

$$k_1 = -0.00266$$

$$k_2 = -652.33$$

TABLE A.14

Coefficients for empirical correlation

$$(Q_A / Q_L) = a \cdot (Q_L / Q_F)^b \cdot (1 - Q_L / Q_F)^c$$

Pipe diameter	Liquid	a	b	c	Multiple correlation
1.0	S2	7.65	0.78	4.64	0.995
1.5	S2	73.60	1.42	16.82	0.981
2.0	S2	257.90	1.52	31.92	0.977
1.0	S1	1.60	0.14	2.43	0.972
1.5	S1	8.83	0.77	11.48	0.929
2.0	S1	77.09	1.27	30.39	0.941
1.0	water	3.84	0.40	4.46	0.998
1.5	water	3.37	0.28	10.65	0.984
2.0	water	25.51	0.78	27.47	0.993

Froude No. (Air) vs Reynolds No. (Liquid)

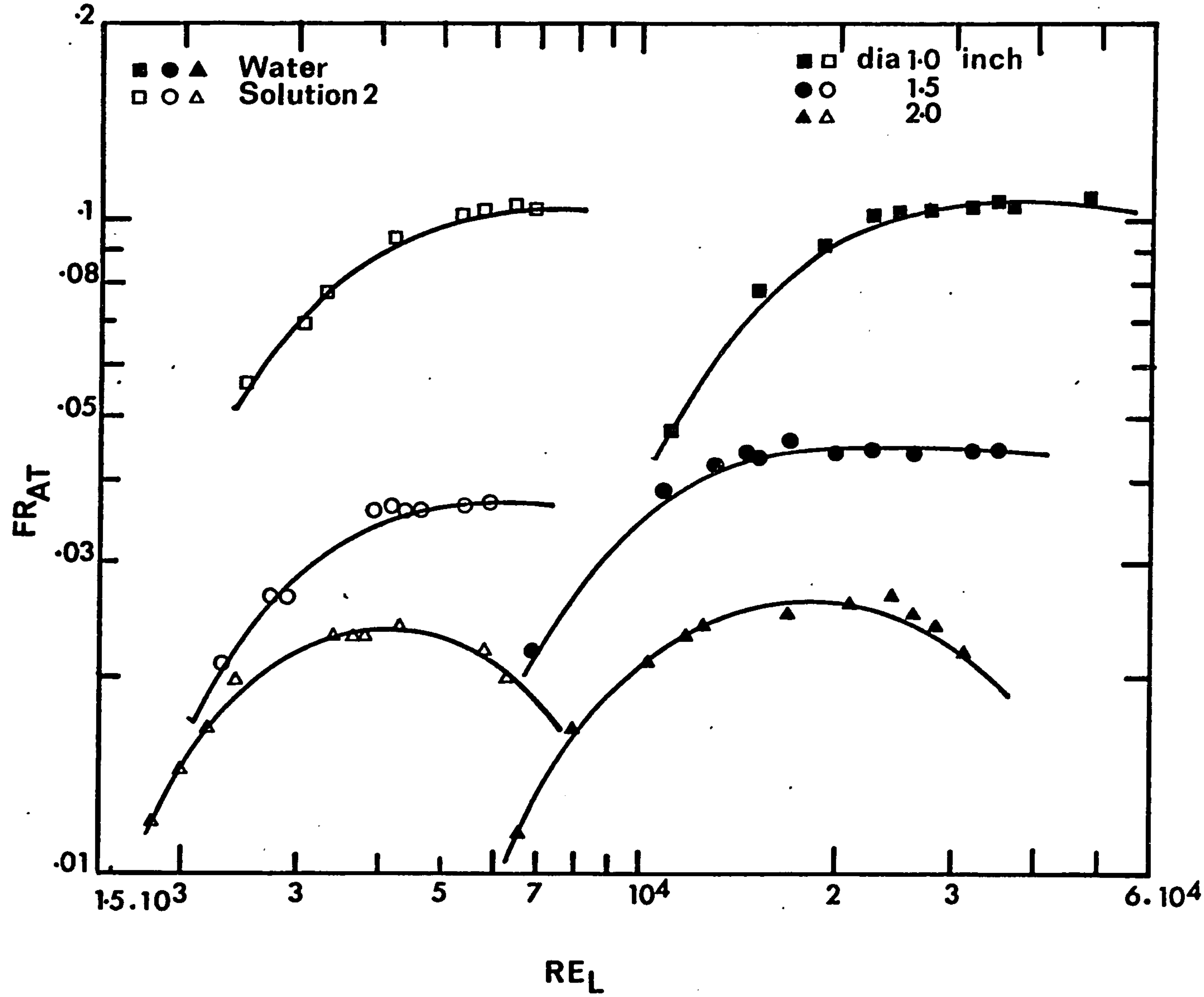

FIGURE A-1

RE_{AT} vs RE_L

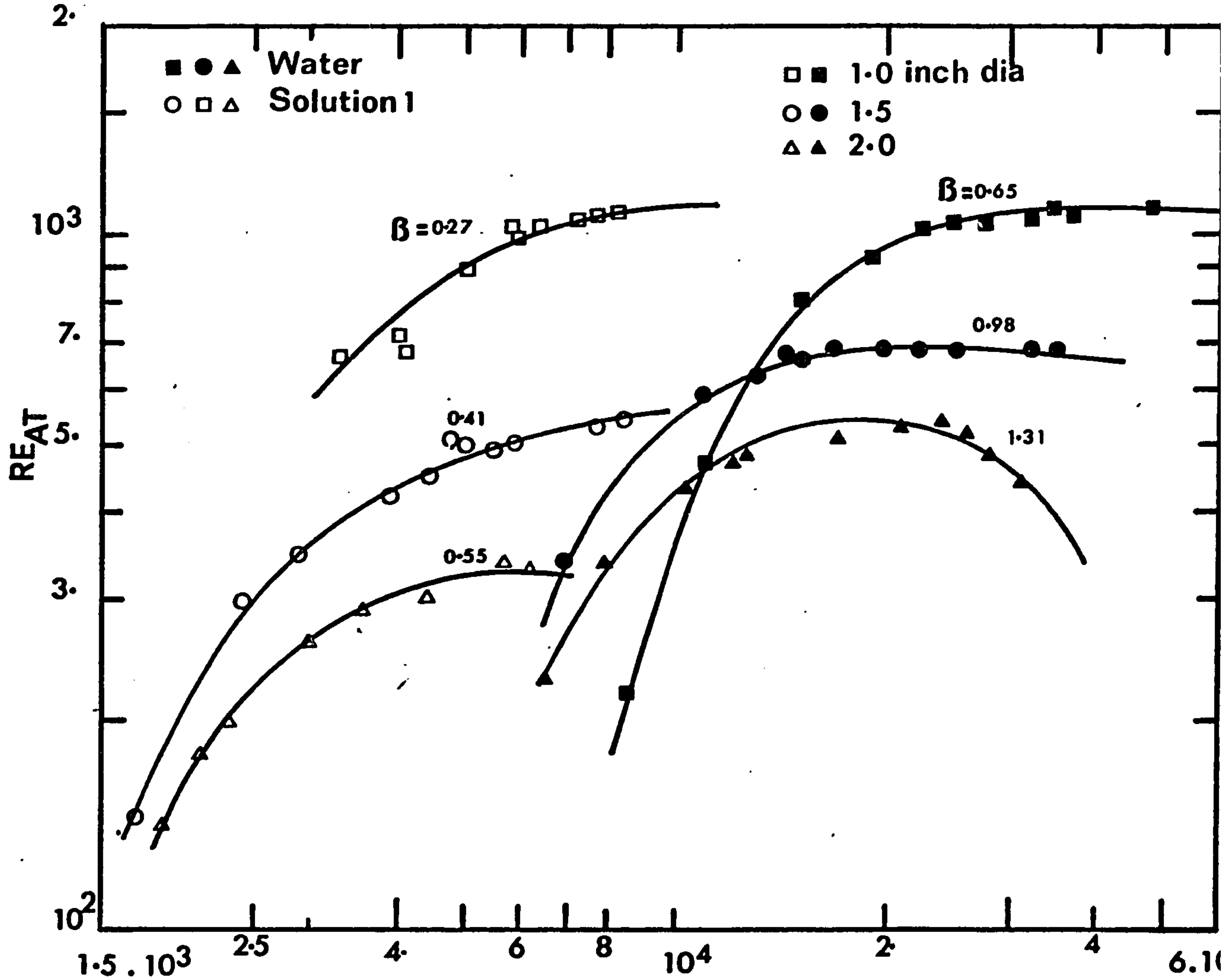

FIGURE A-2

RE_{AT} vs RE_L

Pipe diameter 2·0 inches

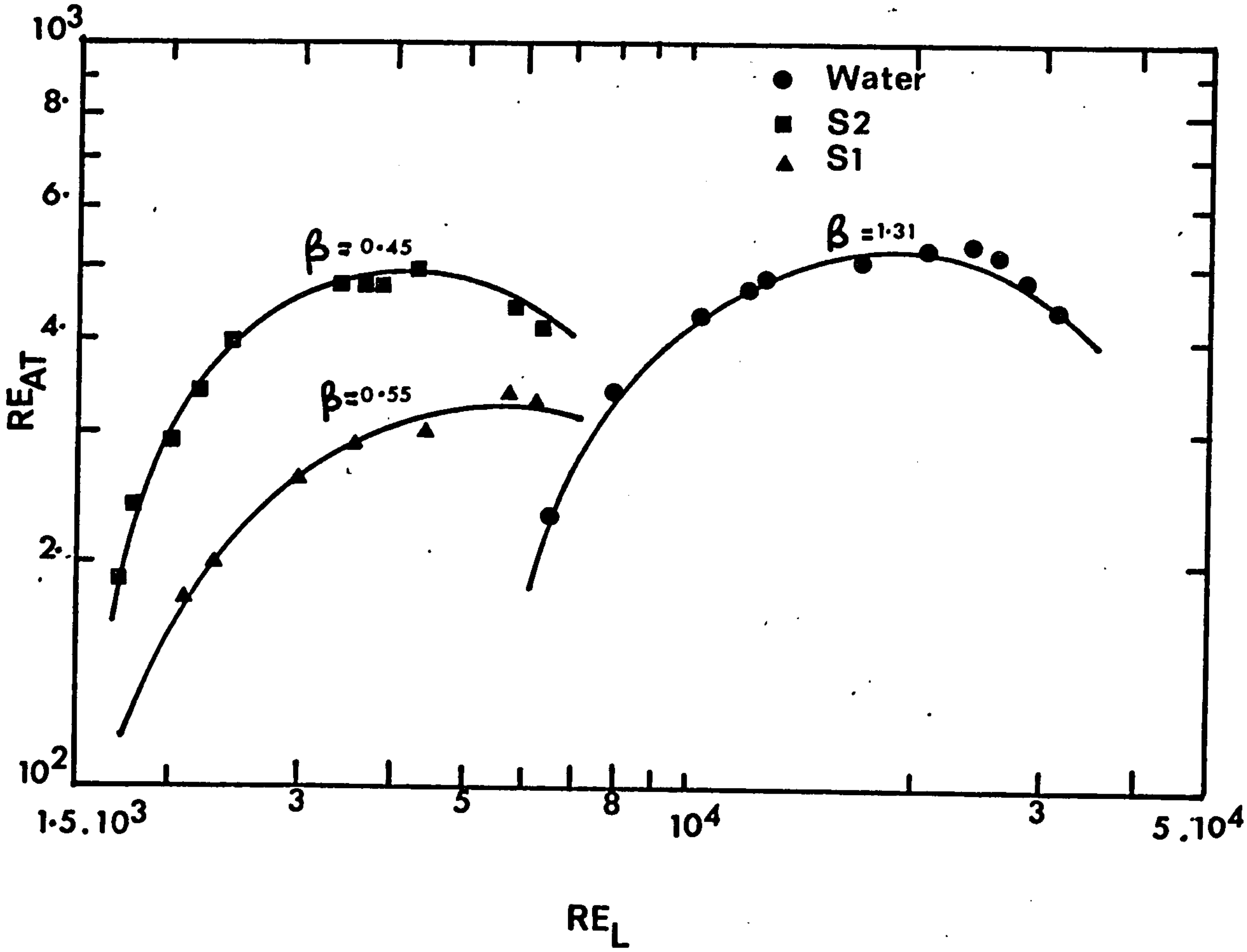

FIGURE A-3

REAT vs REL

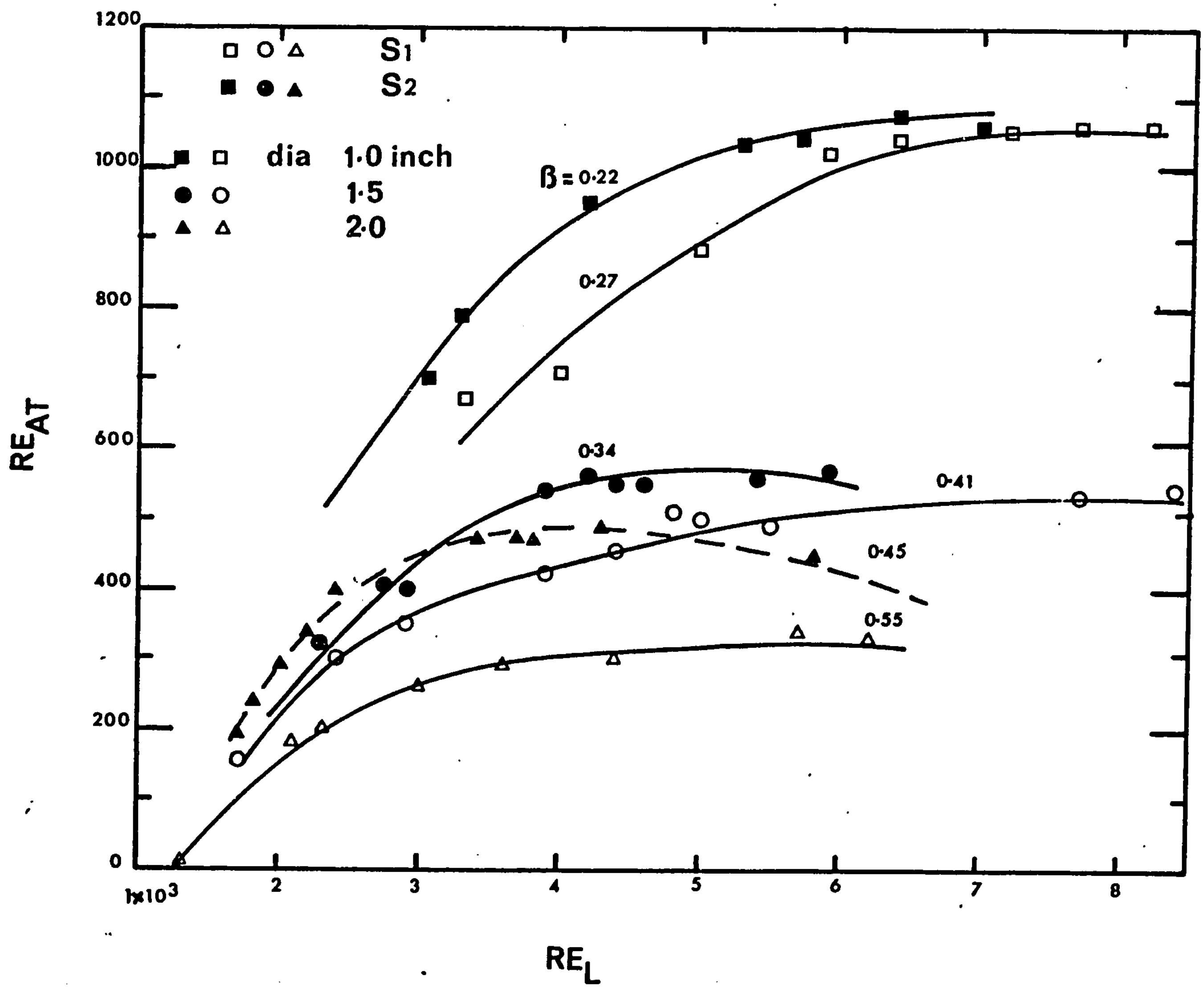

FIGURE A-4

RE_A vs RE_L

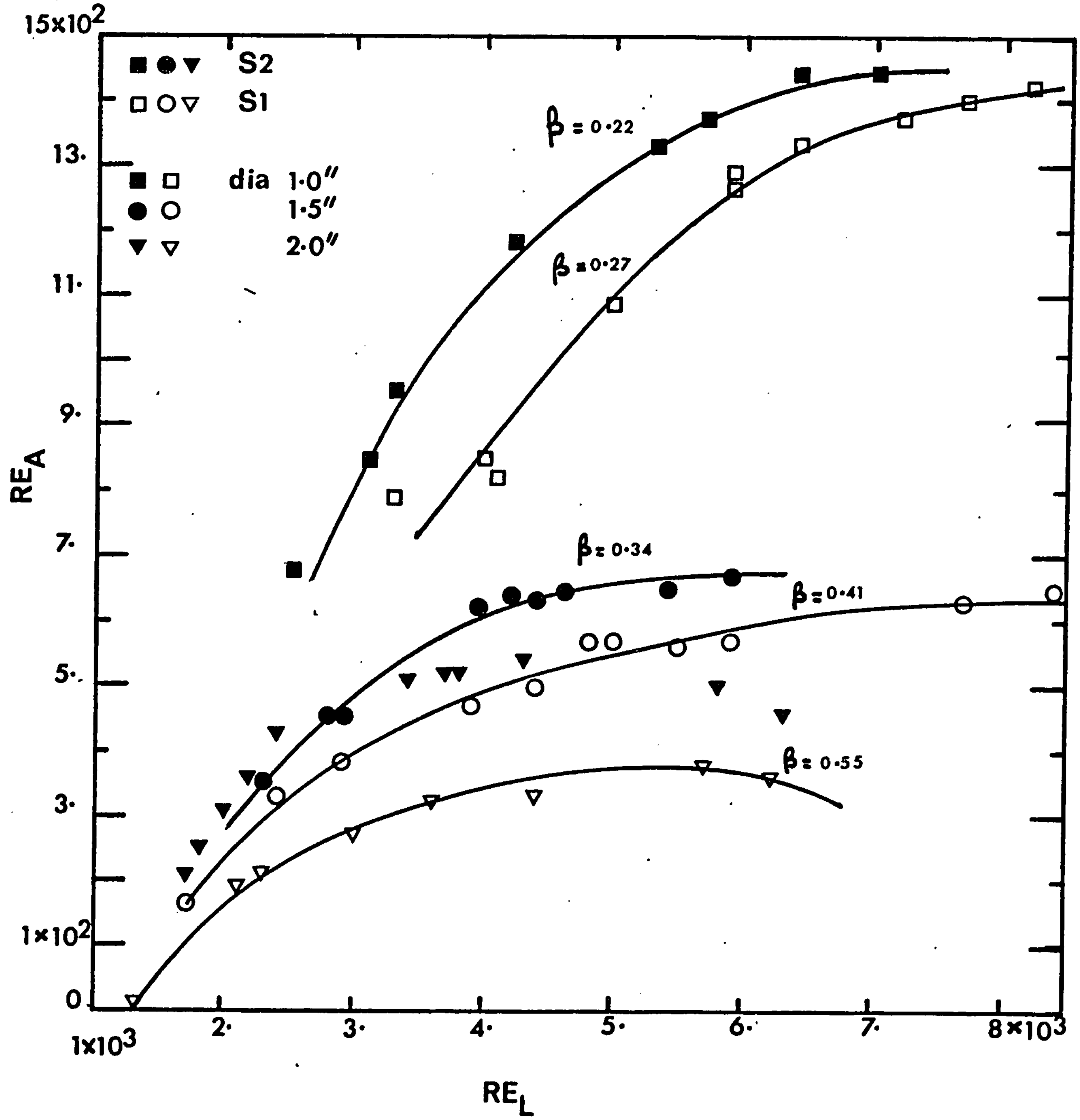

FIGURE A-5

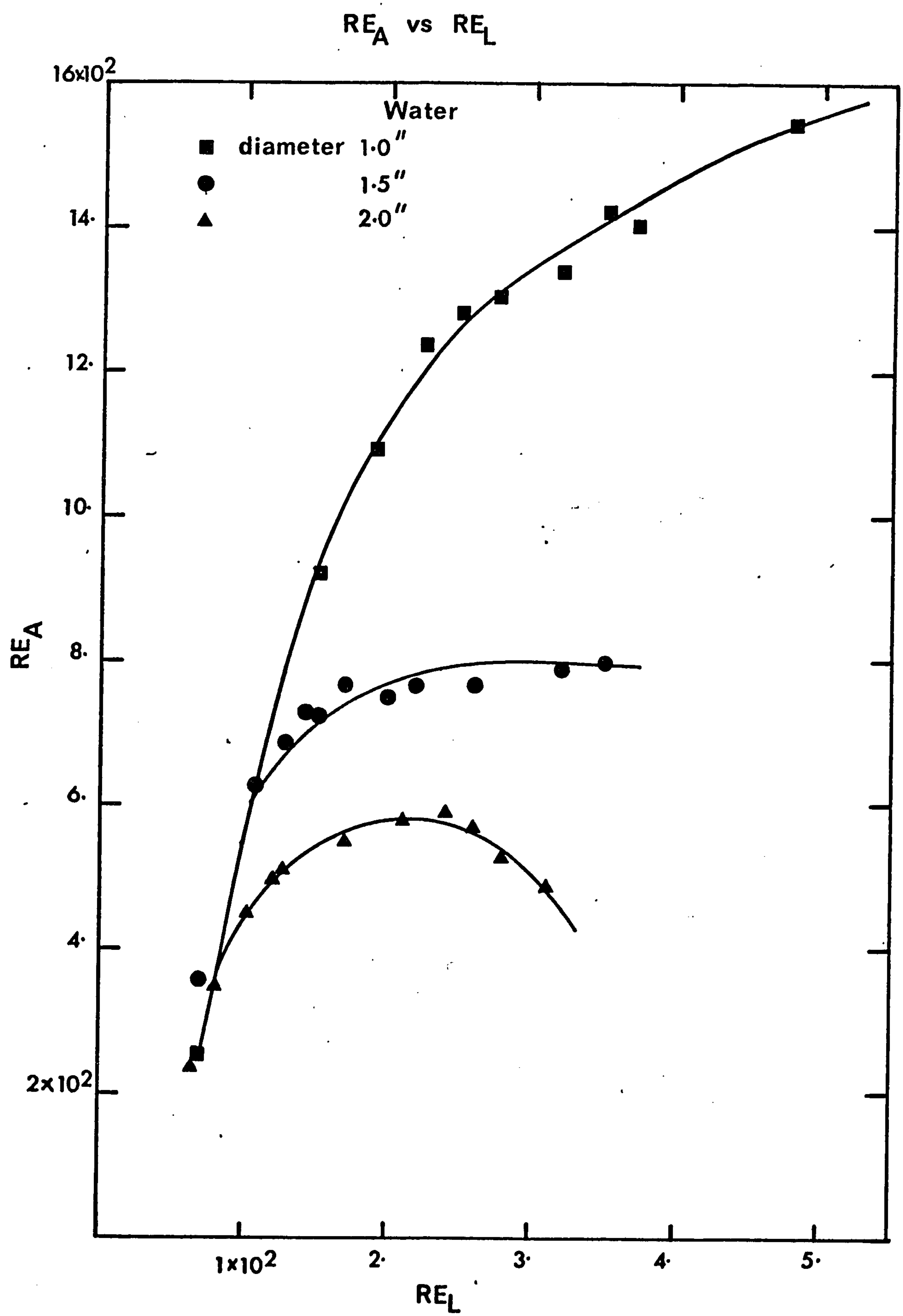
RE_A vs RE_L
16x10^2
14·
12·
10·
8·
6·
4·
2x10^2
RE_A
Water
diameter 1·0″
1·5″
2·0″
1x10^2
2·
3·
4·
5·
RE_L

FIGURE A - 6

RE_A vs RE_I

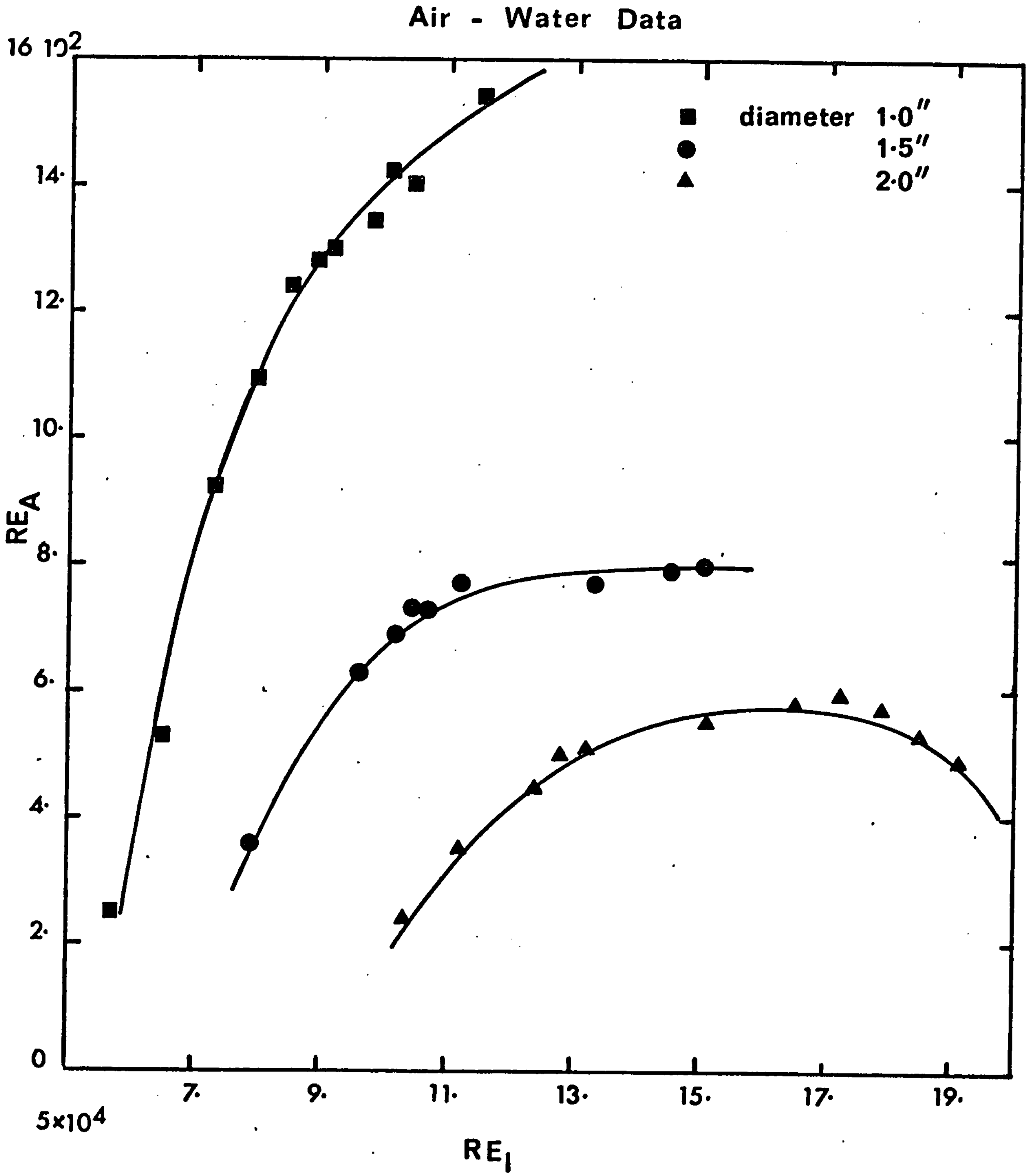

FIGURE A-7

$\pi^2 (V_A/V_l)^2$ vs RE_L

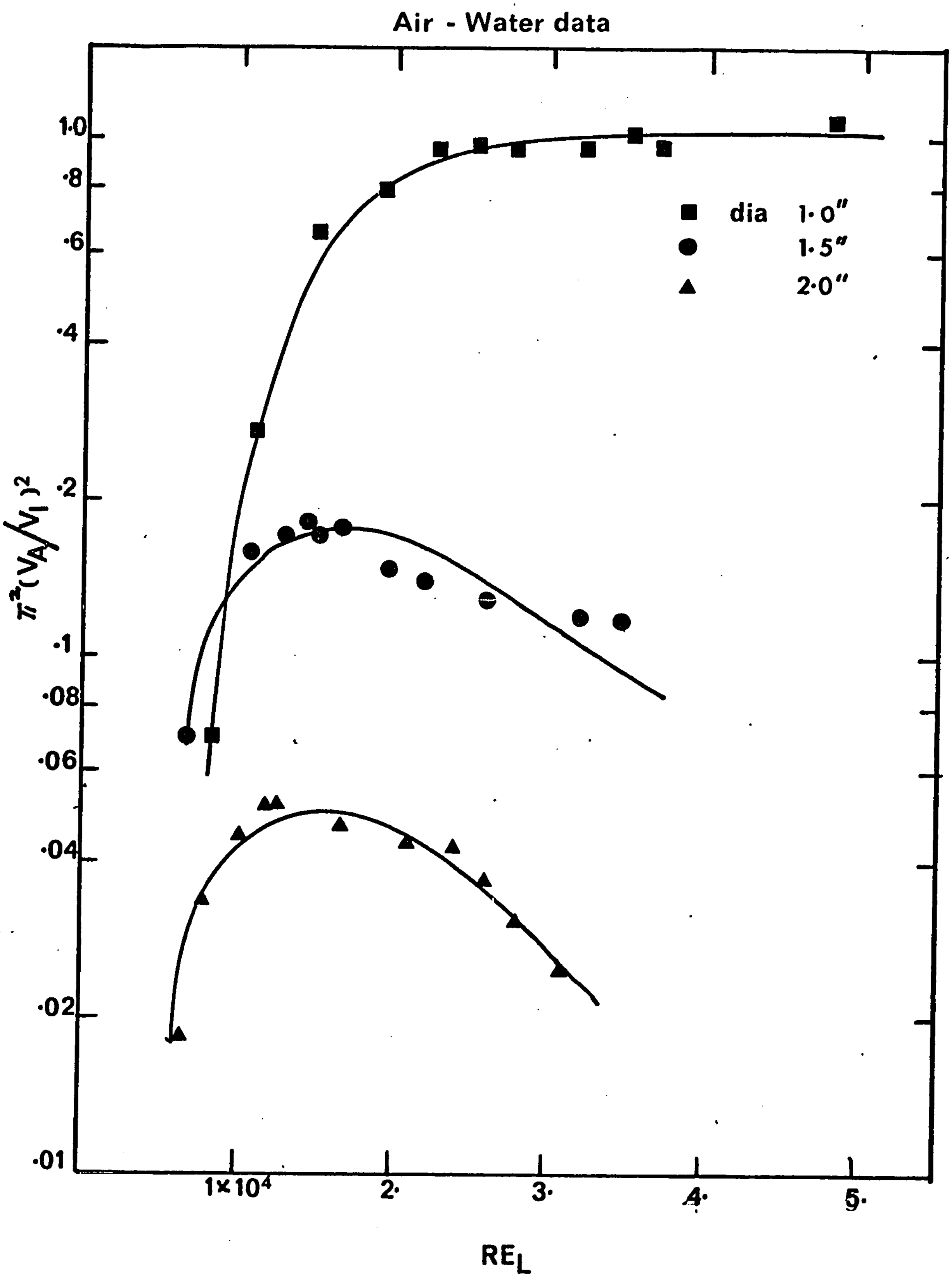

FIGURE A-8